Region-specific maladaptive gray matter myelination is associated with differential susceptibility to stress-induced behavior in male rodents and humans

Kimberly L. P. Long, Ph.D.[1,†], Linda L. Chao, Ph.D.[2-3], Yurika Kazama, B.A.[1], Anjile An, M.P.H.[1,4], Kelsey Y. Hu[1], Lior Peretz, B.A.[5], Dyana C. Y. Muller, B.A.[6], Vivian D. Roan, B.A.[1], Rhea Misra, B.A.[1], Claire E. Toth[1], Jocelyn M. Breton, Ph.D.[1,Ψ], William Casazza, B.S.[7], Sara Mostafavi, Ph.D.[7,8], Bertrand R. Huber, M.D., Ph.D.[9,10], Steven H. Woodward, Ph.D.[11], Thomas C. Neylan, M.D.[3,12], Daniela Kaufer, Ph.D.[1,8,13]*

[1]Helen Wills Neuroscience Institute, University of California, Berkeley, Berkeley, CA 94720, USA.

[2]Department of Radiology & Biomedical Imaging, University of California, San Francisco, San Francisco, CA 94143, USA.

[3]Department of Psychiatry and Behavioral Sciences, University of California, San Francisco, San Francisco, CA 94143, USA.

[4]Division of Biostatistics, Department of Population Health Sciences, Weill Cornell Medicine, New York, NY 10065, USA

[5]Department of Molecular, Cellular, and Developmental Biology, University of California, Los Angeles, Los Angeles, CA 90095, USA.

[6]Department of Computer Science, University of Arizona, Tucson, AZ 85721, USA.

[7]Department of Statistics and Department of Medical Genetics, University of British Columbia, Vancouver, BC V6T 1Z4, Canada.

[8]Canadian Institute for Advanced Research, Toronto, ON M5G 1M1, Canada.

[9]Department of Neurology, Boston University, Boston, MA 02215, USA.

[10]National Center for PTSD, VA New England Health Care System, Boston, MA 02130, USA.

[11]National Center for PTSD, VA Palo Alto Health Care System, Palo Alto, CA 94304, USA.

[12]San Francisco VA Health Care System, San Francisco, CA 94121, USA.

[13]Department of Integrative Biology, University of California, Berkeley, Berkeley, CA 94720, USA.

*To whom correspondence should be addressed: danielak@berkeley.edu, (510) 642-9346

†Current address: Department of Psychiatry and Behavioral Sciences, University of California, San Francisco, San Francisco, CA 94143, USA.

ΨCurrent address: Department of Psychiatry, Columbia University, New York, NY, 10027, USA.

Running Title: Regional myelin is associated with stress susceptibility.

Keywords: Stress, avoidance, oligodendrocytes, myelin, hippocampus, amygdala

Abstract

Background

Individual reactions to traumatic stress vary dramatically, yet the biological basis of this variation remains poorly understood. Recent studies have demonstrated surprising plasticity of oligodendrocytes and myelin in the adult brain, providing a potential mechanism by which aberrant structural and functional changes arise in the brain following trauma exposure.

Methods

We tested the hypothesis that gray matter myelin contributes to traumatic stress-induced behavioral variation. We exposed adult rats to a single, severe stressor and used a multimodal approach to characterize avoidance, startle, and fear-learning behavior. We quantified oligodendrocyte and myelin content in multiple brain areas and compared these measures to behavioral metrics. We then induced overexpression of the oligodendrogenic transcription factor Olig1 in the adult rat dentate gyrus (DG) to test the potential, causal role of oligodendrogenesis in behavioral variation. Lastly, T1-/T2-weighted estimates of myelin were compared to trauma-induced symptom profiles in humans.

Results

Oligodendrocytes and myelin in the DG of the hippocampus positively correlated with stress-induced avoidance behaviors in male rats. In contrast, myelin levels in the amygdala positively correlated with contextual fear learning. Olig1 overexpression increased place avoidance compared to control virus animals, indicating that increased oligodendrocyte drive in the DG is sufficient to induce an avoidance behavioral phenotype. Finally, variation in myelin correlated with trauma-induced symptom profiles in humans in a region-specific manner that mirrored our rodent findings.

Conclusions

These results demonstrate a species-independent relationship between region-specific, gray matter oligodendrocytes and myelin and differential behavioral phenotypes following traumatic stress exposure. This study provides a novel biological framework for understanding the mechanisms that underlie individual variance in sensitivity to traumatic stress.

Introduction

Exposure to a traumatic stressor induces a spectrum of outcomes in both humans and animals, ranging from no apparent changes in behavior to long-lasting changes across different behavioral domains (1–5). In humans, persistent, trauma-induced changes to avoidance-, fear-, and arousal-related behaviors define the psychiatric criteria for anxiety or post-traumatic stress disorder (PTSD) (6,7). Interestingly, not all who experience trauma will develop subsequent mood or anxiety disorders (2–5); however, the underlying physiological mechanisms of selective susceptibility and resilience to trauma are poorly understood. Furthermore, biomarkers of susceptibility along with novel therapeutic targets for anxiety and PTSD are sorely lacking.

Recent studies have uncovered a surprising role for oligodendrocytes and the myelin they produce in experience-dependent plasticity and behavior (8–12), suggesting that myelination may be a novel mechanism by which stress produces adverse psychiatric outcomes (10,13). Interestingly, axonal input and hormonal signaling can induce proliferation of oligodendrocyte precursor cells (OPCs) and remodeling of existing myelin (14–19). This plasticity has causal effects on behaviors such as motor function, spatial memory consolidation, and motor learning (14,20,21), suggesting that adult myelin plasticity in gray matter regions is necessary for proper synaptogenesis, circuit function, and learning. In addition, oligodendrocytes are sensitive to various environmental stressors. These cells express glucocorticoid receptors throughout their lineage (22,23), and stressors affect oligodendrocytes and myelin in a region-specific manner (24–28). For example, chronic stress decreases myelin density in the prefrontal cortex (PFC) (29–31), and early weaning in mice increases myelin production in the amygdala (32). Furthermore, we have previously shown in adult male rats that chronic stress or exposure to stress-level glucocorticoids increases oligodendrogenesis from neural stem cells in the dentate gyrus (DG) of the hippocampus (33).

Oligodendrocyte and myelin plasticity may ultimately contribute to fear learning and affective behavior in both rodents and humans. For example, conditional ablation of OPCs in the PFC increases anxiety-like behavior and decreases social behavior in mice (34), and inhibiting new myelination in mice impairs remote fear memory recall (26). Furthermore, growing evidence suggests that oligodendrocyte plasticity contributes to stress outcomes and psychiatric disorders in humans (35–46). Specifically, early life stressors such as institutionalization and neglect alter white matter microstructure in the PFC, and these alterations are correlated with PFC-related cognitive deficits (39). Patients with major depressive disorder display changes to white matter in the frontal-limbic system that correlate with behavioral symptoms such as rumination (41,42,46). Beyond white matter, recent evidence has raised the intriguing possibility that myelination in gray matter regions, such as the amygdala and hippocampus, plays a role in psychiatric disorders (44,47). Namely, patients with major depressive disorder display decreased oligodendrocyte cell

densities in the amygdala (44). Furthermore, we have shown that patients diagnosed with PTSD have significantly higher myelin content in the hippocampus as compared to trauma-exposed subjects without PTSD, and hippocampal myelin levels positively correlate with PTSD symptom severity (47). This suggests that oligodendrocytes and myelin in gray matter regions may correspond to individual differences in trauma-induced psychiatric pathology.

Given the sensitivity of oligodendrocytes to neuronal activity and stress, coupled with the alterations to oligodendrocytes and myelin seen in various psychiatric disorders, these cells are poised to contribute to the adverse behavioral outcomes of trauma. The current study unites these two concepts in an explicitly translational design. First, in a rodent model of exposure to a single, acute trauma, we performed microstructural analyses of oligodendrogenesis in relation to quantitative measures of avoidance, startle, and contextual fear memory. We then conducted Olig1-driven gain of function in the hippocampus to test whether altering oligodendrocyte content within the hippocampus is sufficient to induce a behavioral phenotype in the absence of stress exposure. In humans, we extended our original analysis of myelin in the brains of human veterans by including the amygdala and analyzing domain-specific CAPS data.

Materials and Methods

Study design

The aim of this study was to determine the relationship between oligodendrocytes, myelin, and the behavioral outcomes of trauma. Rodents were exposed to an acute, severe stressor, and outcomes were assessed using behavioral (avoidance, fear, and startle assays) and molecular (immunofluorescent staining) measures. An experimental gain-of-function (Olig1 upregulation) was used to investigate whether oligodendrogenesis contributes to behavioral outcomes. Translatability of these findings was further supported by complementary measures of myelin in human subjects (via T1-/T2-weighted MRI imaging) and their comparison to sub-components of the Clinician Administered PTSD Scale. The experimental designs and methodology of outcome measures were chosen prior to initiating each experiment. For all experiments, subjects were randomly assigned to experimental groups. Investigators were blind to stress and virus condition during behavioral assays and data quantification. The criteria for animal exclusion were surgical complications and unsuccessful viral targeting; otherwise, no animals were excluded from analyses. Study design and sample sizes used for each experiment are provided in figure legends.

Animals

All animal care and procedures were approved by the University of California, Berkeley, Institutional Animal Care and Use Committee. A total of 70 adult (P65) male Sprague Dawley rats were

purchased from Charles River and pair-housed on a 12:12 light-dark cycle (lights on at 0700 hours) in our facility at UC Berkeley. Rats had *ad libitum* access to food and water and were given one week to acclimate to the facility before testing began. Rats underwent gentle handling (being picked up and held) for 5 days prior to stress (Fig. 1A). All animals were weighed on the third day of handling. For the first study (Fig. 1A), 40 male animals were used (20 control and 20 stress). For the fear conditioning study (Fig. 3A), 12 males were used. Finally, for the viral work (Fig. 4B), 18 male rats were used.

Stress

To establish a rodent model with which to study acute, severe trauma exposure, we coupled a single exposure to predator scent (fox urine) with 3 hours of immobilization in adult, male Sprague-Dawley rats. Rats were randomly assigned to undergo stress or remain in the home cage. Rats were run in pairs in cohorts of 10 animals each, with numbers of control and stress animals counterbalanced between cohorts. In the stress group (n = 20), rats underwent acute immobilization stress with exposure to predator scent. Cage mates were placed side-by-side in an empty cage inside a fume hood from 0900-1200 hours while being restrained in Decapicone bags (Braintree Scientific, Braintree, MA). A cotton ball infused with 1 mL of fox urine (Trap Shack Co. Red Fox Urine, amazon.com) was placed in the center of the cage. Tail vein blood was collected from stress-exposed rats at 0 minutes, 30 minutes, and 3 hours into acute immobilization stress. After cessation of stress, animals were injected with BrdU (detailed below) and were released and returned to a clean cage to allow for self-grooming. After 1 hour, rats were returned to a clean home cage. Rats in the control group (n = 20) received BrdU injections and a cage change at the same time of day.

BrdU injections

To quantify oligodendrogenesis following acute stress exposure, rats were injected intraperitoneally with 100 mg/kg 5-Bromo-2′-deoxyuridine (BrdU, Sigma-Aldrich, St. Louis, MI) dissolved in warm 0.9% saline immediately after release from Decapicone bags. They were then injected once each day for the following two days within one hour of the circadian time of the first injection. Control animals were injected at similar times of the day, taking care to avoid transfer of fox and stress odors.

Behavioral battery

Animals underwent a behavioral battery 7 days after stress exposure to characterize the extent of persistent behavioral changes. All behaviors were conducted between 0800-1400 hours. Prior to all tests, animals were brought to the testing space and allowed at least 30 min to acclimate. One day prior to stress, all animals went through a 5 min baseline open field test (OFT) under dim lighting (15 lux). Seven days after acute immobilization stress, all rats were individually profiled for anxiety-like behaviors using 6

different behavioral tests: OFT in a brightly lit environment (OFT Light), OFT in a dimly lit environment (OFT Dim), light/dark box (LD), elevated plus maze (EPM) in a bright environment, EPM in a dim environment, and acoustic startle response (ASR). Low light versions of the OFT and EPM were utilized as low anxiogenic versions of their full light counterparts, allowing for further characterization of exploratory and anxiety-like behavior. The battery spanned two days with the following sequence: Day 1 -- OFT Light, EPM Light, ASR; Day 2 – OFT Dim, LD, EPM Dim. After placing an animal into an arena, the experimenter exited the room. Animals were given 10 minutes of rest in the home cage in between each test. Of note, our behavior facility underwent construction over the course of this study, and our apparatuses were moved to a new suite after experiment 1 (corresponding to Figs. 1 and 2). Subsequent behavior tests (corresponding to Fig. 4) were conducted in new rooms under identical conditions, except for the EPM Dim, in which dim red light was substituted for dim white light.

Open field test (OFT)

Each rat was placed in an unenclosed plastic box (50 w x 50 l x 58 h in cm) and was given 10 minutes to explore the arena. All animals were placed along a wall at the beginning of the test. Behavior was recorded with cameras positioned above the arena and connected to GeoVision software (GeoVision Inc., Taiwan). Behavior was scored as latency to, frequency, and total amount of time spent in the center of the box (designated by a 15 x 15 cm square) EthoVision software (Noldus, Leesburg, VA). In addition, we quantified the duration of rearing (upright posture with both forepaws lifted off the ground) and self-grooming from the OFT Light. The OFT Light was conducted under full lighting (280 lux). The OFT Dim was conducted in a different but identically structured box in the same room under 15 lux. The arena was cleaned with 1% acetic acid followed by Formula 409 All Purpose Cleaner after each animal.

Elevated plus maze (EPM)

Rats were allowed to explore an EPM for 10 min (arm dimensions: 10 w x 60 l in cm; closed arm enclosed by walls 51 cm in height; apparatus elevated 50 cm off the ground). Behavior was recorded by a JVC Everio camera (JVCKENWOOD, Tokyo, Japan) mounted above the apparatus. The criterion for open arm exploration was considered as more than half of the body (and both forepaws) placed into the open arm. Latency to and total time spent in the exposed open arms, as well as time spent in the protected closed arms, were quantified by observers blind to condition. The EPM Light was conducted at 240 lux, while the EPM Dim was conducted at 125 lux. The apparatus was cleaned with 1% Process NPD Disinfectant (STERIS Life Sciences) after each animal.

Light-dark box (LD)

Each rat was placed in a structure consisting of an enclosed dark box separated by a divider with a small door leading to an unenclosed light box (each box 15 w x 15 l x 8 h in inches). All animals were placed into the dark half of the box and given 10 min to explore. Behavior was recorded by a JVC Everio camera (JVCKENWOOD, Tokyo, Japan) mounted above the apparatus. Measures for latency to, frequency, and total time spent in the exposed side were quantified via EthoVision software or observers blind to condition. The arena was cleaned with 70% ethanol after each animal.

Acoustic startle response (ASR)

Each rat was placed into an isolated Coulbourn sound-attenuating fear conditioning chamber (12 w x 10 l x 12 h in inches) and was exposed to 5 min of background noise (~55 dB). This was followed by 70-110 dB white noise pulses lasting 10 ms, with an inter-stimulus interval of 15-30 s. All tones were calibrated with a handheld decibel meter each day prior to testing. Behavior was recorded over two different trials: habituation (110 dB tones presented 15 times to assess initial responses and subsequent habituation) and threshold determination (70-110 dB tones presented in pseudo-random order, with each tone played 5 times in total). Behavior was recorded using a Coulbourn Instruments camera connected to a computer with FreezeFrame software (Coulbourn Instruments, Whitehall, PA). The boxes were cleaned with 70% ethanol after each animal. Startle behavior was assessed by EthoVision software analysis of activity change (measured as percent pixel change from frame to frame). The amplitude of startle was quantified as the maximum activity minus baseline activity in the 50 ms surrounding the startle pulse. From the habituation phase, we quantified initial startle (mean startle amplitude to stimuli 1-3); final startle (mean startle amplitude to stimuli 13-15); mean startle (mean of all startle amplitude scores across all 15 stimuli); and sensitization, calculated as 100*(final startle - initial startle)/(initial startle). Habituation is, therefore, Sensitization*(-1). From the threshold phase, we averaged startle scores from the 5 presentations of each of the decibel levels (70, 80, 90, 100, and 110 dB) to generate a startle threshold curve for each animal, and we quantified the area under the curve (AUC).

Composite behavior scoring

To standardize and quantify behavior across multiple behavior tests, we adapted the method of Cutoff Behavioral Criteria developed by Cohen and Zohar (48). For each measure, a behavioral cutoff criterion was defined by the 20th percentile of the control distribution. For measures in which greater scores indicate greater anxiety-like behavior (latency to an anxiogenic zone, time spent in an anxiolytic zone), the 80th percentile of the control group was used. Binary scoring was applied: Animals falling outside the criterion were marked as “affected” and received a score of 1 for that measure. Scores were then summed across all tests. High scores represent consistent anxiety-like behavior across all tests. We compared these

scores to 3 other methods of composite scoring: Z scoring, principal component analysis (PCA), and ranks. For Z scoring, we converted all measures to Z scores using the mean and standard deviation of the control group; Z scores were then averaged across all measures from all tests. For PCA, we conducted a PCA on all measures from all animals via custom Python scripts and recorded each animal's value from the first principal component. For ranks, for each measure, we sorted all animals in ascending order and assigned each animal a rank for that measure from 0 (least anxiety-like behavior) to 40 (highest anxiety-like behavior). For example, the animal with the least time spent in the center of the OFT receives a rank of 40. Ranks were then averaged across all measures from all tests. Each of these composite scoring methods (Z scores, first principal component values, and average ranks) were compared to composite cutoff scoring via Pearson correlations.

Fear conditioning cohort

A separate cohort of 12 male rats was used to test repeated avoidance profiling coupled with fear conditioning. All animals underwent a one-day profiling battery consisting of the OFT Light, EPM Light, and LD with 10 minutes in the home cage in between each test (day -19 relative to stress). Eight days later (day -11), the animals went through a second one-day behavior profiling battery. Rats went through the acute, severe stress paradigm (day 0) with blood sampling 11 days later, followed by a third avoidance profiling battery 7 days later (day +7). On day +8 post-stress, all animals underwent a 3-day fear conditioning protocol. On the first day, animals were placed in a Coulbourn sound-attenuating fear conditioning chamber (12 w x 10 l x 12 h in inches) with an electrified grid floor. Animals were allowed 5 min to acclimate to the box. Following acclimation, 10 unsignaled, 1 mA, 1 s duration shocks were delivered with an inter-stimulus interval of 15-120 s. Rats were left in the chamber for 3 min after the last shock and then returned to the home cage. On the second day (day +9), animals were placed back into the fear context without shock and underwent 5 extinction trials lasting 10 min each. Inter-extinction trial intervals were ~90 min. On the third day (day +10), animals were again placed in the fear context without shock for a single 10 min extinction-retention test (Probe). The fear chamber was cleaned with 70% ethanol in between each animal. The time spent freezing in each trial was quantified by observers blind to condition. Extinction was quantified as area under the curve (AUC) from the 5 extinctions trials. Animals underwent the ASR test on day +11, and on day +14, animals underwent a final 15 min LD test prior to perfusion 15 min later.

Perfusion

Rats were deeply anesthetized with Euthasol Euthanasia Solution (Virbac AH, Inc.) and transcardially perfused with 0.9% saline followed by ice-cold 4% paraformaldehyde (PFA) in 0.1 M

phosphate-buffered saline (PBS). Brains were post-fixed for 24 hours at 4°C in 4% PFA and equilibrated in 30% sucrose in 0.1 M PBS. They were then stored at -80°C. The brains were sliced into free-floating 40 µm sections on a cryostat in a 1 in 12 series and were subsequently stored at -20°C in antifreeze solution.

Immunohistochemistry and fluorescence microscopy

Immunomarkers for immature to mature, myelinating oligodendrocyte cell bodies [glutathione S-transferase pi (GSTπ) and carbonic anhydrase II (CAII)] and myelin basic protein (MBP) were selected for quantification. Immunohistochemical staining was conducted over a 2-day period. On the first day, slices were blocked with 3% normal donkey serum (NDS) in tris-buffered saline (TBS) with 0.3% Triton-X100 for one hour at room temperature. The slices were then incubated overnight at 4°C in blocking solution with primary antibodies. Primary antibodies were rat anti-MBP (1:500; Abcam, Cambridge, UK), rabbit anti-GSTπ (1:1000; MBL International, Woburn, MA), and sheep anti-CAII (1:10000; AbD Serotec, Hercules, CA). On the second day of staining, the slices were rinsed and incubated in fluorophore-conjugated secondary antibodies for 2 hours at room temperature in blocking solution. Secondary antibodies were Alexa Fluor 647 donkey anti-sheep (Jackson ImmunoResearch, West Grove, PA), Cy3 donkey anti-rat (Jackson ImmunoResearch, West Grove, PA), and Alexa Fluor 488 donkey anti-rabbit (Jackson ImmunoResearch, West Grove, PA). Lastly, the sections were stained with the nuclear marker DAPI. Stained sections were mounted onto glass slides and coverslipped with DABCO antifading medium.

Imaging of slides was conducted under a 40x objective using a Zeiss 510 AxioImager microscope (Zeiss, Oberkochen, Germany) with MetaMorph software (Molecular Devices, San Jose, CA) and a 10x air objective on a Zeiss AxioScan Slide Scanner (AxioScan.Z1, Zeiss, Oberkochen, Germany) with Zen software (Zeiss). Regions of interest were scanned and automatically stitched. For the DG, sections from Bregma -2.9 to -5.28 were imaged, and the granule cell layer (GCL) and hilus (defined as the region within the GCL blades and medial to the stratum pyramidale of CA3) were traced. Cells were counted from 4-8 hemispheres of the dorsal DG from each animal with Fiji software (Fig. 2B) (49). Overall DG measures were collected by summing measures from the hilus and GCL. For other brain regions, ROIs of standardized size (75 x 75 µm to 300 x 300 µm) were collected from both hemispheres of 2-6 sections (Fig. 2B). Cell bodies were counted via automated thresholding and particle analysis in Fiji, and output was visually confirmed by observers blind to condition. This allowed for high throughput cell counting from many regions. For all regions, myelin content was measured from the raw images by the integrated fluorescence intensity of MBP immunofluorescence. All measures for all regions were averaged across sections and normalized to area in mm^2 (cell densities) or μm^2 (MBP intensity).

Olig1 lentivirus and stereotaxic injections

To test whether hippocampal oligodendrogenesis contributes to avoidance behavior, two 3rd generation lentiviral expression vectors were designed with VectorBuilder (Santa Clara, CA). The control vector was designed to express enhanced green fluorescent protein (EGFP) under the human cytomegalovirus (CMV) promoter (Fig. 4A). The experimental vector was a bicistronic design with the CMV promoter driving expression of mouse Olig1 (NM_016968.4) followed by a second CMV promoter driving EGFP. Plasmids were packaged by the UC Berkeley High Throughput Screening Facility in HEK293T cells. Cells were transfected via jetPRIME (VWR, Radnor, PA) with the viral plasmid and 3 helper plasmids (pCMV-VSVG, pMDL, and pRSV-Rev). The resulting virus-containing media was collected 48 h and 72 h after transfection. Virus was precipitated with 5% PEG and 0.15M NaCl and centrifuged at 3000 g for 15 min at 4°C. The precipitated viral pellet was resuspended in ice cold phosphate-buffered saline (PBS), aliquoted, and stored at -80°C. Viral titer was determined with an ABM qPCR Lentivirus Titration Kit (ABM, Vancouver, B.C., Canada). Titers were 10^6-10^7 infectious particles/mL.

For viral injections into the DG, animals were injected with 0.05 mg/kg buprenorphine and anesthetized with isoflurane (2-3%). Using a stereotaxic frame, bilateral craniotomies were made at the following coordinates: -3.5 mm anterior/posterior, +/-2.2 mm medial/lateral relative to bregma, and -3.3 mm relative to dura. For viral infusion, 1.3 µL of virus was infused at a rate of 0.1 µL/min into each hemisphere. After the injection, the needle was left in place for five minutes to allow for viral diffusion, then was slowly removed to minimize viral infection along the needle tract. One animal from the Lenti-Olig1 group was removed from further analysis due to unilateral injection failure. One animal from the Lenti-GFP control group was removed for post-surgical complications (chronic swelling around the wound site).

MRI Data Acquisition and Processing

For complete methods, see Chao et al., 2015 (47). Briefly, magnetic resonance imaging (MRI) was performed on 38 male veterans (19 PTSD+, 19 PTSD-) at the Center for Imaging of Neurodegenerative Diseases at the San Francisco Veterans Affairs Medical Center. Participants were evaluated by a clinician to determine exposure to trauma events. Participants were ruled out for drug use or dependence within the last six months, alcohol use or dependence within the last twelve months, or a history of bipolar or psychotic disorders. PTSD symptoms were assessed using the Clinician Administered PTSD Scale (CAPS).

The MRI scans were acquired using a Bruker/Siemens Med-Spec 4T MRI system (Bruker BioSpin, Ettlingen, Germany). The scans acquired included a T1-weighted magnetization prepared gradient echo sequence and a volumetric T2-weighted turbospin echo sequence. The images were processed and assessed for myelination levels using the methods outlined by Chao et al., 2015 (47). The FreeSurfer version 4.5 tissue boundary delineations were used to assign the regions of interest (50).

Statistical Analysis

All data are presented as mean ± standard error of the mean (SEM). Other than 2 animals excluded from the virus cohort for surgical complications, all data points are included; no outliers are excluded. Two sample comparisons were performed by two-tailed student's t-test, and multiple group comparisons were conducted by ANOVA, followed by Tukey's post-hoc testing to compare individual groups when a main effect was detected. Greenhouse-Geisser corrections were used when the assumption of sphericity was broken, as indicated by Mauchly's test of sphericity. To compare the relationships between measures, we conducted Pearson correlations. In all tests, the alpha value was set at 0.05. Analyses were performed using IBM SPSS 19 (SPSS, Inc., Chicago, IL) and GraphPad Prism version 8.0.0 for Mac OS X (GraphPad Software, San Diego, California USA, www.graphpad.com). Hierarchical clustering was performed in Python. For human work, statistical analysis was performed on the demographic, descriptive, and clinical characteristics across the groups using both the student's t-test for continuous variables and the Fisher's exact test of independence for categorical variables. The relationship between PTSD symptom severity (i.e., CAPS) and hippocampal myelin content was examined with Spearman's Rank-Order correlation.

Results

Exposure to acute, severe stress yields a spectrum of anxiety-like behavior in adult male rats

We first sought to determine the relationship between oligodendrocytes, myelin, and the behavioral outcomes of trauma in a rodent model. To establish a rodent model with which to study acute, severe trauma, we coupled a single exposure to predator scent (fox urine) with 3 hours of immobilization in adult, male Sprague-Dawley rats (Fig. 1A). Predator scent is a potent stressor with ethological validity in rodents. When coupled with immobilization, predator scent is a severe stressor that elicits a large corticosterone response in the rat (51–53). We subjected a group of male rats to stress (n = 20), while a second group served as controls and remained minimally disturbed in their home cages (n = 20).

Following acute trauma exposure in rodents and humans, the majority of individuals gradually recover to baseline levels of fear and anxiety, while a subset of susceptible individuals displays persistent changes to behavior (4,48). To identify stress-susceptible rats, we allowed animals to remain in the home cage with minimal disturbance for 7 days after stress. We then characterized the extent of behavioral changes with a battery of tests spanning the behavioral domains of exploration, avoidance, startle, and ethologically-defined anxiety-like behavior (rearing and grooming) (Fig. 1B). This paradigm identifies a sub-population of stress-exposed animals displaying persistent and stable changes to anxiety-like behavior (48,54,55). Behavioral assays included the open field test (OFT) under highly anxiogenic (brightly lit: OFT

Light) and low anxiogenic (dimly lit: OFT Dim) conditions, elevated plus maze (EPM) under bright and dim conditions, light-dark box test (LD), and acoustic startle response (ASR) test. For OFT, EPM, and LD tests, we quantified frequency, duration, and latency of visits to anxiogenic and anxiolytic zones (Supplementary Fig. 1). In addition, we quantified rearing and grooming behavior from the OFT Light, both of which have been used as ethological measures of general anxiety-like behavior in the rat (56,57). From the ASR test, we quantified an individual's habituation (and, conversely, sensitization) to repeated startle stimuli, mean startle response, and startle response curve to tones of increasing decibels (58).

Stress-induced changes to behavior may be isolated to a single domain or coordinated across multiple domains (5,59,60). To determine how behavioral domains relate to each other in our acute stress paradigm, we characterized the correlations of the behavioral measures within and across assays (Fig. 1C). Interestingly, in control animals, avoidance assays showed several cross-assay correlations to startle measures, but not to exploration measures. Conversely, in stress-exposed animals, avoidance assays showed cross-assay correlations to exploration, but not startle, measures. The rodent-specific anxiety-like measures of rearing and grooming showed no strong relationships to measures from other domains in either control or stress-exposed groups.

These observations were confirmed by unbiased hierarchical clustering analyses (Fig. 1D and E). In the control group, the first order branching yielded 2 clusters. Control Cluster 1 consisted of all OFT measures and grooming behavior, while Control Cluster 2 consisted of all avoidance and startle measures, as well as rearing behavior. In the stress group, the first order of branching again yielded 2 clusters; however, cluster membership was altered compared to controls. Stress Cluster 1 consisted of all OFT measures and all avoidance measures (except 2 latency measures -- EPM Light latency to the open arm and OFT Dim latency to the center). These 2 latency measures resided in Stress Cluster 2 with all startle measures, as well as rearing and grooming behavior. Together, this reveals that acute stress exposure shifts behavioral patterns. In stress-exposed animals, open field behavior aligns with measures of avoidance. This suggests that the OFT resembles an approach/avoidance conflict assay only in animals exposed to stress. Furthermore, in our model, avoidance and startle were not strongly correlated after acute stress exposure.

Clinical scores such as the CAPS provide a numeric value that encapsulates many individual, yet related, measures, providing greater weight than a single measure in isolation. Here, we sought to model the CAPS in this rodent model by generating a comprehensive score for behavior across all tests. To do this, we adapted the concept of Cutoff Behavioral Criteria to assign a numerical score for each anxiety-like behavioral measure (Supplementary Fig. 2) (48,58). Briefly, quantitative measures were compared to the control group distribution and given a binary score of 0 or 1 depending on whether they fall below a cutoff criterion, defined here as the 20th percentile of the control group (Supplementary Fig. 1 and Supplementary Fig. 2A-B). This cutoff was chosen to capture animals with the most extreme behavioral responses and to

model the prevalence rates of high anxiety behavior seen in rats and human clinical populations (61). Scores are then summed across all measures (Supplementary Fig. 2C). High scores on this scale reflect that an animal consistently displayed anxiety-like behavior across many measures and assays when compared to control animals. Similar methods have been used to classify rats subjected to predator exposure, and a recent study used cutoff scoring to classify distinct behavioral phenotypes in mice subjected to chronic unpredictable stress (60,62). Here, we found that cutoff-based composite scores were strongly correlated with values from 3 separate methods of quantifying individual variability: Z scoring, principal component analysis, and averaging ranks across measures, providing further validity for this technique (Supplementary Fig. 2D-F). Using this scoring method, we found that stress-exposed males displayed a wide range of composite scores (Fig. 2A). There was a trend towards higher mean composite behavior scores in the stress group as compared to controls ($p = 0.06$) (Fig. 2A). Stress-exposed animal scores spanned across the full range from minimally affected (composite score = 2) to highly affected (composite score = 19), enabling us to investigate factors that contribute to resilience and susceptibility to anxiety-like behavior after stress.

Anxiety-like behavior correlates with mature oligodendrocyte and myelin content in the DG of stress-exposed animals.

We have previously shown that exposure of male rats to chronic stress or 7 days of corticosterone injections increases oligodendrogenesis in the DG of the hippocampus (33). Although the behavioral consequences of this increase in the rat brain are unknown, recent studies provide hints that myelin and oligodendrocytes in gray matter regions may contribute to stress-induced behavioral phenotypes (27,34). For example, we demonstrated that human subjects diagnosed with PTSD have significantly higher hippocampal myelin content as compared to trauma-exposed subjects without PTSD (47). Moreover, myelin levels in the hippocampus correlated with CAPS scores, such that greater myelin levels corresponded to worse symptom scores (47). We sought to test whether this relationship holds true in a controlled animal model. We hypothesized that in the rat model of acute stress exposure, greater anxiety-like behavior after stress would correspond to greater oligodendrocyte and myelin content in the DG. In a subset of animals selected to span the full range of composite scores ($n_{Control} = 12$, $n_{Stress} = 11$), we analyzed cell body immuno-markers of the oligodendrocyte lineage, including the intermediate-to-late-stage marker glutathione S-transferase π (GSTπ), the marker of mature oligodendrocytes carbonic anhydrase II (CAII), and myelin basic protein (MBP) for myelination (Fig. 2B). To determine regional specificity within the hippocampus, we quantified the number of oligodendrocyte cell bodies and myelin staining intensity in the hippocampal granule cell layer (GCL) and hilus (polymorphic layer) of the DG, molecular layer (MoDG), CA3, CA2, CA1, stratum lucidum (SLu), stratum radiatum (Rad), stratum lacunosum moleculare (LMol), and stratum oriens (Or). To further probe specificity between brain regions, we quantified oligodendrocyte

density and myelin staining in the amygdala lateral subdivision (LA), basolateral subdivision (BLA), and central subdivision (CeA), as well as in the brain's major white matter track, the corpus callosum (Fig. 2C).

We then tested our hypothesis that oligodendrocyte measures are correlated with behavioral outcomes. Indeed, we found that in stress-exposed animals, greater oligodendrocyte cell density and greater myelin amounts in the DG of the hippocampus corresponded to greater composite scores of anxiety-like behavior after stress (Fig. 2D-I). A correlation matrix revealed that composite scores of stress-exposed animals correlated with all 3 oligodendrocyte lineage markers in the GCL or hilus (Fig. 2J-L). This is not due to overall increases in oligodendrocyte numbers after stress, as there were no group differences in GSTπ and CAII cell densities or MBP intensity in the DG between control and stress-exposed animals (Supplementary Fig. 3). The positive correlation was specific to the DG; no significant correlations were found for any other region of the hippocampus, amygdala, or corpus callosum in stress-exposed animals. In control animals, MBP in the MoDG and Or were significantly positively correlated with composite scores; however, correlations were not consistent across markers. This suggests that oligodendrocytes and myelin in the DG, but not the amygdala or the corpus callosum, correspond with individual outcomes of anxiety-like behavior after acute stress in male rats.

We then tested which of the two behavioral clusters identified by hierarchical clustering drives the relationship between hippocampal oligodendrocytes and composite behavior scores. In stress-exposed animals, we compared composite scores derived from either Stress Cluster 1 (Avoidance) or Stress Cluster 2 (Startle, Rearing, Grooming) to DG oligodendrocyte and myelin markers. We found significant positive correlations between Stress Cluster 1 composite scores and DG oligodendrocyte and myelin markers that mirrored those of overall scores (Fig. 2M). Stress Cluster 2 composite scores were positively correlated only with CAII in the GCL. Together, these experiments suggest that oligodendrocyte and myelin markers in the hippocampus correspond most strongly with stress-induced avoidance outcomes following exposure to a single, severe stressor in male rats.

Increased myelin content in the amygdala is correlated with enhanced contextual fear learning.

In addition to avoidance behavior and hypervigilance, trauma can alter fear learning and fear extinction (63,64). Thus, we sought to test whether regional oligodendrocytes and myelin also correspond to individual outcomes of fear following exposure to an acute, severe stressor. Furthermore, we hypothesized that baseline behavioral profiles may predict an individual's susceptibility to stress. Thus, we sought to test whether avoidance behavior prior to stress could predict individual outcomes in fear behavior following stress exposure.

To test these hypotheses, we conducted a longitudinal study in which 12 male rats underwent an abbreviated behavioral profiling (OFT + EPM + LD) at 3 time points -- twice before stress (t1 = -19 and t2

= -11 days) and once following stress (t3 = +7 days) (Fig. 3A). To probe for individual variation in fear learning following stress, animals underwent fear conditioning on day +8 after stress (Fig. 3A). Animals displayed a wide variability in time spent freezing across trials (Fig. 3B). We first asked whether avoidance measures prior to and following stress predict these fear measures. A correlation matrix revealed that avoidance measures at t1 (when animals were naïve to behavioral assays) do not predict future fear responses after stress (Supplementary Fig. 4A). Following stress exposure, two measures of boldness (OFT time in center and EPM frequency of open arm entries) negatively correlated with freezing during the first extinction trial (Supplementary Fig. 4B); however, no other avoidance measures correlated with any other measure from fear conditioning. In addition, we compared fear conditioning measures to startle behavior. Two startle measures (initial startle and mean startle) negatively correlated with one fear conditioning measure (freezing during extinction trial 5) (Supplementary Fig. 4C). This suggests that avoidance, startle, and fear are separate domains of behavior in this model.

To test whether oligodendrocytes and myelin correspond to individual differences in fear-like behavior, we quantified oligodendrocyte lineage markers and myelin in the DG of the hippocampus and the sub-regions of the amygdala (Fig. 3A). In the DG, oligodendrocyte cell density and myelin showed no relationships to fear conditioning measures (Fig. 3C). In the amygdala, oligodendrocyte cell density did not correlate with fear conditioning measures (Fig. 3D); however, MBP immunofluorescence (myelin levels) in the LA and BLA subdivisions positively correlated with freezing behavior during extinction trials and AUC of the fear extinction curve (Fig. 3D). Interestingly, LA and BLA MBP measures did not correlate with freezing behavior during initial fear acquisition or during the probe trial. CeA MBP showed similar patterns, though no correlations were statistically significant. Together, these findings indicate that amygdala myelin correlates with extinction freezing behavior, suggesting a potential role for amygdala myelin levels in contextual fear memory following a single, severe stressor in male rats. In addition, avoidance measures before stress do not predict fear-like behavior following stress.

Manipulation of hippocampal oligodendrogenesis mimics stress exposure.

Our results demonstrate hippocampal and amygdala oligodendrocytes and myelin positively correlate with behavioral outcomes in male rats after acute stress exposure. Therefore, we next tested whether manipulating oligodendrocytes is sufficient to induce changes in behavior. Most tools for altering myelin in the rat lead to widespread, rather than regional, changes to myelin (27). To allow for local manipulation of oligodendrocytes, here, we employed a viral vector-mediated approach to induce ectopic overexpression of the oligodendrogenic transcription factor Olig1 in the DG of the hippocampus. We developed a lentiviral construct to drive the expression of Olig1 (*Lenti-CMV-mOlig1-CMV-EGFP*) or GFP control (*Lenti-CMV-EGFP*; Fig. 4A). We designed the viral vector with 2 CMV promoters due to previous

failures of IRES-containing vectors in our animals. We stereotactically delivered virus to the dorsal DG of male rats ($n_{GFP} = 9$, $n_{Olig1} = 7$; Fig. 4A). After six weeks of recovery to allow for viral expression, animals underwent the two-day behavioral profiling protocol as described in Fig. 1B (Fig. 4B).

Viral delivery and expression in the DG were confirmed by GFP expression (Fig. 4C-D). We found that viral expression in Lenti-Olig1 animals was largely restricted to the subgranular zone and molecular layer, with some additional expression in the hilus (Fig. 4C-D). To first confirm effective upregulation of Olig1 expression, we quantified Olig1+ cell density in the GCL and hilus in a subset of animals. We found that rats that received Lenti-Olig1 virus indeed showed significantly more Olig1+ cells in the DG compared to Lenti-GFP animals (Fig. 4E). In order to determine whether Olig1 upregulation altered avoidance behavior, we calculated composite cutoff behavior scores using Lenti-GFP animal behavior as the control distribution. Interestingly, animals that received Lenti-Olig1 virus displayed significantly enhanced anxiety-like behavior scores compared to Lenti-GFP animals (Fig. 4F and Supplementary Fig. 5). In addition, Lenti-Olig1 animals displayed a mean score similar to the stress-exposed animals from cohort 1 (Cohort 1 composite score = 6.6 ± 1.0; Lenti-Olig1 composite score = 9.7 ± 2.0; two-way ANOVA of Cohort and Stress: no significant interaction, $F_{1,52} = 1.69$, $p = 0.20$; no main effect of Cohort, $F_{1,52} = 2.04$, $p = 0.16$; significant main effect of Stress, $F_{1,52} = 10.98$, $p = 0.002$). To determine which behavioral domains were altered by viral delivery, we generated composite scores for avoidance measures and startle measures separately. Lenti-Olig1 animals displayed significantly greater composite avoidance scores than Lenti-GFP animals (Fig. 4G), and these scores were significantly positively correlated with Olig1+ cell density (Fig. 4H), echoing the findings from our first experiment. Interestingly, Lenti-Olig1 animals also displayed greater composite startle scores relative to Lenti-GFP animals (Fig. 4I); however, these scores were not correlated with Olig1+ cell densities (Fig. 4J).

Together, these findings show that Olig1 ectopic overexpression in the dorsal DG increases both avoidance and startle behavior in male rats. Hence, manipulation of the oligodendrocyte population in the absence of exposure to stress was sufficient to phenocopy stress-induced place avoidance and to enhance startle. These findings extend the relationship between hippocampal oligodendrogenesis and behavioral outcomes and suggest that oligodendrogenesis can contribute to the pathogenesis of enhanced stress reactivity.

Hippocampal and amygdala myelin correspond to avoidance and fear in trauma-exposed male veterans.

Previously, we used the ratio of T1-weighted to T2-weighted MRI intensity to estimate gray matter myelin content in a population of 38 male, trauma-exposed veterans (19 diagnosed as PTSD+ and 19 diagnosed as PTSD-) (47). Using these imaging protocols, we showed that hippocampal myelin is positively correlated with overall PTSD symptom severity, as measured by CAPS scores (47). Here, we have now

modeled this relationship in a controlled rodent experiment and extended it to show that oligodendrocytes and myelin in the hippocampus and amygdala correspond in a region-specific manner to individual outcomes of avoidance, startle, and fear-like behavior in male rats exposed to a single, severe stressor. CAPS IV scores encompass symptoms for avoidance (Avoidance sub-score), fear (Re-experiencing sub-score), and hypervigilance (Hyperarousal sub-score) (65). Thus, following our findings in rodents, we hypothesized that estimates of myelin content in the hippocampus and amygdala of male veterans exposed to trauma would regionally correspond to individual outcomes within these categories. To test this, we extended our previous work and correlated myelin estimates from the hippocampus, amygdala, and corpus callosum with individual sub-components of CAPS scores.

As previously shown (47), there is a significant, positive correlation between overall CAPS scores and myelin estimates in the hippocampus (Table 1). Here, we additionally found that myelin estimates from the amygdala, but not the corpus callosum, correlated with overall CAPS scores. When further comparing myelin estimates to categorical sub-scores, we found that both hippocampal and amygdala myelin, but not corpus callosum myelin, were positively correlated with Avoidance and Hyperarousal sub-scores, but not Reexperiencing sub-scores.

We then determined which individual symptoms correspond with myelin levels in the hippocampus, amygdala, and corpus callosum. Here, we found that amygdala and hippocampal myelin estimates displayed divergent relationships with respect to individual PTSD symptoms. Specifically, for individual symptom scores from the Avoidance category, hippocampal myelin estimates positively correlated with place avoidance ("Avoidance of activities, places, people"), while amygdala myelin positively correlated with emotional avoidance ("Avoidance of thoughts, feelings, conversations"). Both regions positively correlated with mood (Hippocampus: "Diminished interest in activities" and "Restricted affect"; Amygdala: "Diminished interest in activities"). In the Reexperiencing category, amygdala myelin was positively correlated with psychological and physiological distress at exposure to cues, while the hippocampus showed no relationship to any symptom. In the Hyperarousal category, hippocampal myelin positively correlated with sleep disruption ("Difficulty sleeping"), irritability ("Irritability, frequency"), and concentration ("Difficulty concentrating"), but not with startle measures. In contrast, amygdala myelin estimates were positively correlated with startle ("Exaggerated startle response"), but not with sleep disruptions, irritability, or concentration. Interestingly, corpus callosum myelin estimates showed no significant relationships to any CAPS measures, a finding consistent with our rodent work.

In sum, hippocampal myelin in trauma-exposed men positively correlated with individual outcomes relating to place avoidance and hyperarousal, while amygdala myelin correlated with individual outcomes surrounding cue-associated distress, emotion, and startle. Both regions correlated with aspects of mood, and the corpus callosum, the brain's largest white matter tract, showed no relationship to any aspects of

PTSD symptomology. Together, these findings mirror several aspects of our rodent work. They provide clinical relevance to our findings and point to future avenues of investigation.

Discussion

This study was motivated by the unmet critical need to understand the neural mechanisms that drive behavioral variation in response to acute, traumatic stress. Here, we identified region-specific gray matter oligodendrocytes and myelin as correlative indicators and potential contributors to avoidance behavior and fear learning after stress. Our findings provide a novel biological framework to understand how individual variance in persistent sensitivity to traumatic stress arises. In this study, we used a multimodal method of quantifying behavior to demonstrate that acute, severe stress yields individual variation in anxiety-like and fear behavior in male rats. We found that persistent increases in place avoidance were positively correlated with hippocampal oligodendrocyte and myelin measures, while individual outcomes of contextual fear learning were positively correlated with amygdala myelin measures. Together, these findings suggest that oligodendrocytes and myelin in these regions correspond with differential susceptibility to stress. Indeed, driving oligodendrogenesis in the hippocampus was sufficient to enhance avoidance behavior in the absence of a stressor. Similarly, MRI-based estimates of gray matter myelin in trauma-exposed, male veterans positively correlated with PTSD symptomology in a region-specific manner: hippocampal myelin corresponded with place avoidance, and amygdala myelin corresponded with cue-associated fear.

While many studies approach stress susceptibility and resilience from the lens of chronic stress, far fewer utilize an acute, severe stressor. Yet, many traumatic stressors, such as car accidents, physical assault, and shootings, can be acute events that trigger long-lasting changes to the brain and behavior (66). Modeling exposure to acute, severe stress, then, is critical to understanding the mechanisms of susceptibility to trauma. Here, we utilized a rat model in which animals were exposed to 3 hours of immobilization with simultaneous exposure to fox odor; this is an inescapable stressor that our lab has shown to be more severe than immobilization alone (53). To evaluate rodent behavior after acute stress in a way that models the complex and variable human outcomes, we utilized a multivariate approach to quantify exploration, avoidance, hypervigilance behavior, fear learning, and fear extinction. We found that the behavioral domain of avoidance clustered with exploration, but not startle, after acute stress. Fear conditioning behavior also did not strongly correlate with avoidance or startle measures. This may speak to the separability of these domains and/or the specificity of behavioral changes induced by our paradigm.

In this work, we developed composite cutoff behavior scoring to characterize behavioral profiles in rats. This method, and the Cutoff Behavioral Criteria from which it was adapted, does not rely upon absolute values of behavior, but instead applies binary scoring after application of a cutoff; this method is

modeled upon human clinical standards and previous work with the method of Cutoff Behavioral Criteria (58,67,68). With this, summing scores from many measures and many assays allows for identification of animals that consistently display anxiety-like behavior. Similar thresholding techniques have been used to define distinct behavioral phenotypes in animals exposed to acute or chronic stress (60,69). In our study, this method revealed that one week after acute stress exposure, animals display a spectrum of scores, from minimally affected to highly affected. Unlike the discrete nature of diagnoses, the effects of trauma are not binary (66); therefore, our approach models the continuous nature of stress effects and provides another means with which to investigate the physiological, neural, and glial factors that correspond with and contribute to the continuum of anxiety-like behavior. These results also reveal the limitations of considering the mean scores of group performance, as these statistical measures mask the true effect on the individual studied.

A growing number of studies implicate myelin and oligodendrocytes in behavioral outcomes associated with stress (10,13,30). These studies have generally utilized chronic stress paradigms and have shown that chronic stress decreases myelin in regions such as the PFC or in white matter tracts (24,25). Here however, we showed that two weeks after an acute stressor, greater myelin in the hippocampus corresponded with greater avoidance behavior, and greater myelin in the amygdala corresponded with greater contextual fear learning. These findings add an important dimension to a growing body of literature which demonstrates that oligodendrocytes outside of white matter tracts are associated with behavioral outcomes following stress exposure and other experiences. Indeed, experience and neural activity induce oligodendrogenesis and myelination in regions such as the PFC and premotor cortex, and manipulating oligodendrogenesis and myelination can alter motor learning, fear recall, and social behavior (14,21,26,34). Our work expands upon such results by detailing additional gray matter regions in which oligodendrocytes may influence behavior; specifically, we implicate oligodendrocytes and myelin in the hippocampus and amygdala in anxiety-like phenotypes following stress exposure. In addition, our data support and expand upon a recent study that utilized microarray gene expression data from animals exposed to acute stress, which demonstrated that hippocampal oligodendrocyte proportions are elevated in animals displaying PTSD-like behavioral responses (70). Here, we find similar increases in oligodendrocyte density in the hippocampus of animals with high composite anxiety-like behavior scores. We further demonstrate a correlative relationship between behavioral outcomes and hippocampal oligodendrocyte content, we provide evidence suggesting a causal relationship between the two, and we demonstrate the clinical relevance of this phenomenon.

Interestingly, in our study, hippocampal and amygdala myelin displayed unique relationships to the behavioral domains of avoidance, startle, and fear. Specifically, oligodendrocytes and myelin in the DG of the hippocampus positively correlated with avoidance behavior, but not to overall startle or fear. This may

suggest that oligodendrocytes in the DG are specifically associated with the hippocampal functions of exploratory drive and behavioral inhibition (71,72). In the amygdala, myelin in the lateral and basolateral subdivisions correlated with freezing behavior during fear extinction trials, but not overall avoidance or startle behavior. This may suggest that myelin in these amygdalar regions enhances contextual fear memory, perhaps via crystallization of associative learning or via enhancement of efferents that contribute to the amygdala's control of behavior. Future work should seek to incorporate other hippocampal- and amygdala-specific behavioral tasks that show deficits in PTSD-related behavior, such as spatial navigation tasks or cued fear learning (73,74), in order to elucidate how region-specific myelin measures correspond to the full array of trauma-induced behavioral outcomes.

Several studies have demonstrated that targeted disruption of oligodendrogenesis yields behavioral effects on learning and depression-like behavior, suggesting that these cells are active contributors to circuit function (21,34). Hence, our findings may suggest that increased myelin content in the hippocampus and amygdala affects these regions' function in such a way as to contribute to anxiety-like behavior. However, the functional roles of oligodendrocytes and myelin in the hippocampus and amygdala are poorly understood. First, little is known regarding the nature of myelinated axons in the amygdala. Long-range afferents to and efferents from amygdalar nuclei are myelinated (75,76); however, whether oligodendrocytes myelinate short-range axons within the amygdala and what the function of such myelination may be are questions that remain largely unexplored. Second, in the DG, mossy fibers are typically unmyelinated (77). Instead, studies from human brains suggest that the myelinated fibers of the hilus consist of long-range projections of the medial septum, locus coeruleus, and the raphe nuclei (78,79). This leads to several hypotheses regarding our findings. First, given that the medial septum is believed to contribute to hippocampal theta activity (80), increased myelination of these fibers could alter hippocampal rhythms, which may then alter overall hippocampal function. Second, the locus coeruleus provides noradrenergic input to the DG, primarily along the mossy fiber path (78). Emotional arousal stimulates locus coeruleus activity, and noradrenaline has been implicated in emotional memory (81,82). Therefore, increased myelination of these axons could enhance noradrenergic signaling and synaptic plasticity in the hippocampus to enhance anxiety-like behavior. Finally, the median raphe nucleus provides serotonergic input to the DG (83,84). Hippocampal serotonin has been extensively studied for its role in stress and depression (85); therefore, enhanced myelination of these inputs could affect hippocampal serotonergic tone and hippocampal function. Lastly, beyond the expected effects of changes in myelination to conduction velocity, neural synchrony, and millisecond axonal precision, oligodendrocytes have also been shown to alter synaptic function locally, providing an additional mechanism by which increased oligodendrocyte density may alter hippocampal function and anxiety-like behavior (86–90). Parsing these hypotheses with ultra-resolution imaging techniques is a critical next step for this work.

The correlations observed here among oligodendrocyte numbers, myelination, and behavioral outcomes may reflect different biological scenarios. First, baseline variation in the density of oligodendrocytes and myelin may confer variable sensitivity to stress exposure. Second, variability in physiological stress responses may confer variation in the regulation of oligodendrogenesis. Selecting between these hypotheses will require quantification of oligodendrocytes and myelin *in vivo* in a longitudinal design, utilizing methods such as imaging with small mammal MRI or temporally-controlled genetic techniques to label new myelin that still allow for behavioral profiling.

An additional question that then arises is whether the correlation of oligodendrocytes to behavioral outcomes is merely an epiphenomenon (implying the potential to serve as a biomarker for vulnerability to stress-induced anxiety) or whether increased oligodendrogenesis plays a driving role in the pathogenesis of stress-induced anxiety outcomes (implying the potential to serve as a therapeutic target). Our gain-of-function experiment demonstrates that driving oligodendrogenesis in the DG is sufficient to bring about increased avoidance and startle behavior. This moves our findings beyond correlational work and suggests that hippocampal oligodendrogenesis can contribute to anxiety-like behavior. Of note, we chose a constitutive promoter that could target multiple cell types, but a clear limitation of this approach is the non-specificity of transgene expression. In addition, loss-of-function experiments are needed to address the question of necessity, which may ultimately contribute to the development of pharmacological interventions for trauma-induced disorders. Lastly, we focused our gain-of-function experiment on the hippocampus, but future work should seek to conduct additional gain- and loss-of-function experiments in sites such as the amygdala and corpus callosum. Nonetheless, this experiment further adds to the growing body of work demonstrating that adaptive myelination is not a passive epiphenomenon but a contributing factor to experience-dependent plasticity and neural circuit function in the context of stress.

In this study, we employed a translational approach, in which our results from human studies informed our experiments with rodents and vice versa. Hence, following the finding of a positive relationship between hippocampal and amygdala myelin with avoidance and fear behavior in the rat, we turned to a group of trauma-exposed veterans to determine the relationship between region-specific myelin estimates and individual components of PTSD symptom profiles (47). We demonstrated that estimates of hippocampal myelin in trauma-exposed veterans correlate with place avoidance, sleep disturbances, and concentration. In contrast, amygdala myelin correlated with cue-associated distress, emotional avoidance, and exaggerated startle. This adds a comparative and translational perspective to our rodent findings. For example, we saw parallels between rodents and humans in the relationship between hippocampal myelin and avoidance and between amygdala myelin and contextual fear. These parallels imply that such relationships between gray matter myelin and behavior are evolutionarily conserved and species-independent. In addition, they emphasize that relationships between myelin and individual domains of

symptoms and behavior are region-specific. In contrast, rodents and humans differed in how startle behavior related to amygdala myelin, with humans exhibiting positive correlations between amygdala myelin and startle, and rodents exhibiting no such correlations. Incorporating additional behavioral paradigms and expanding analyses to brain-wide circuits in both rodents and humans are needed to build a comprehensive model of how myelin relates to behavioral vulnerability following exposure to a traumatic stressor. Notably, our findings in humans emphasize additional areas of interest for future research in rodent models. For example, sleep disturbances were highly correlated with hippocampal myelin in veterans; future work should, therefore, seek to determine whether stress-induced oligodendrogenesis and myelination in the hippocampus alter sleep patterns in rodents. Ultimately, this study represents an example of an expressly translational investigation in which similar brain regional biomarkers are correlated with nominally analogous behavioral indices across rats and humans. While studies of this kind inevitably highlight the incongruities facing the translational enterprise as regards species differences, sample homogeneities, and methods of assessing biomarkers and behaviors, testing the framework in this manner still has great potential for enhancing our understanding of the etiology of neuropsychiatric disorders.

An unresolved consideration of our study is the question of sex differences. Interestingly, preliminary data from our lab suggest that female rats are resilient to this same acute, severe stress paradigm (unpublished data). In human clinical populations, including our own, a scarcity of female veterans who meet all study criteria precludes meaningful analyses in women. Hence, the relationship between myelin and stress-induced behavior in female populations remains limited. Given the hypothesized sex differences of psychiatric and behavioral outcomes in women and female rodents after stress (91–93), future studies should seek to explore these relationships in female populations utilizing stressors and assays tuned to female behavior.

This study presents important insight for the understanding of psychiatric disorders. Abnormalities in myelin and oligodendrocytes have been implicated in numerous disorders, including PTSD, depression, schizophrenia, autism, and Alzheimer's disease (10,46,47,94–97). Our findings here suggest a role for gray matter oligodendrocytes and myelin in selective susceptibility to stress-induced anxiety, adding to the growing hypothesis that myelin in the CNS contributes to the pathophysiology of psychiatric conditions. Ultimately, while molecular phenotyping of tumor markers transformed the field of cancer diagnosis and treatment, the field of psychiatry is lagging far behind any promise of personalized medicine. By identifying regional relationships between myelin and behavior, our findings may ultimately lead to much needed imaging-based tools for mechanism-based patient stratification that will aid in identifying and treating the most vulnerable individuals.

Acknowledgments: We thank Ellen Brooker, Linnea Delucchi, Brian Gallagher, Natalie Musick, David Seo, Chau Pham, Lydia Ross, Katerina Alexander, Anjana Krishnamurthy, and Cory Berg for assistance with animal work, imaging, and cell counting. Slide imaging experiments were conducted at the Cancer Research Laboratory Molecular Imaging Center, supported by the UC Berkeley Biological Faculty Research Fund. We would like to thank Holly Aaron and Feather Ives for their microscopy training and assistance. We thank Mary West, Pingping He, and the UC Berkeley QB3 Cell & Tissue Analysis Facility / High-Throughput Screening Facility for lentiviral packaging. **Funding**: This research was supported by NIMH R01MH115020 (D.K. and T.C.N.), a NARSAD independent investigator award (D.K.), a Canadian Institute for Advanced Research fellowship (D.K.), an NSF GRFP (K.L.), an American Association of University Women American Dissertation Fellowship (K.L.), and an NSERC-CREATE grant (W.C.). **Author contributions**: D.K. and K.L. devised experiments. K.L. performed experiments and analyses. L.L.C. conducted and analyzed human MRI. Y.K., A.A., K.H., L.P., D.M., V.R., R.M., C.T., and J.B. performed animal work, immunohistochemistry, and analysis. W.C. and S.M. provided oversight and support for statistical analyses. B.R.H. and S.H.W. supervised human PTSD analyses. T.C.N. and D.K. directed the project. K.L., Y.K., D.M., L.P., and D.K. wrote the manuscript. **Conflict of Interest**: The authors declare no conflicts of interest. **Data and materials availability**: All data associated with this study are available in the main text or the supplementary materials.

Supplementary Materials

Supplementary Fig. 1: Measures from behavior profiling tests.

Supplementary Fig. 2: Composite cutoff scoring.

Supplementary Fig. 3: Acute, severe stress does not alter DG oligodendrocyte and myelin content.

Supplementary Fig. 4: Longitudinal relationships between avoidance, startle, and fear conditioning behavior.

Supplementary Fig. 5: Behavioral measures from avoidance tests in Lenti-GFP vs. Lenti-Olig1 animals.

References:

1. McEwen BS, Stellar E (1993): Stress and the Individual: Mechanisms Leading to Disease. *Arch Intern Med* 153: 2093–2101.
2. Kessler RC (1995): Posttraumatic Stress Disorder in the National Comorbidity Survey. *Archives of General Psychiatry* 52: 1048.
3. Kolk BA van der (1988): The trauma spectrum: The interaction of biological and social events in the genesis of the trauma response. *J Trauma Stress* 1: 273–290.
4. Yehuda R, LeDoux J (2007): Response Variation following Trauma: A Translational Neuroscience Approach to Understanding PTSD. *Neuron* 56: 19–32.
5. Yehuda R, Hoge CW, McFarlane AC, Vermetten E, Lanius RA, Nievergelt CM, *et al.* (2015): Post-traumatic stress disorder [no. 1]. *Nature Reviews Disease Primers* 1: 1–22.
6. American Psychiatric Association (2013): *Diagnostic and Statistical Manual of Mental Disorders (5th Ed.)*, 5th ed. Retrieved from https://doi.org/10.1176/appi.books.9780890425596
7. Kirkpatrick HA, Heller GM (2014): Post-Traumatic Stress Disorder: Theory and Treatment Update. *Int J Psychiatry Med* 47: 337–346.
8. Almeida RG, Lyons DA (2017): On Myelinated Axon Plasticity and Neuronal Circuit Formation and Function. *The Journal of Neuroscience* 37: 10023–10034.
9. Fields RD (2005): Myelination: an overlooked mechanism of synaptic plasticity? *The Neuroscientist : a review journal bringing neurobiology, neurology and psychiatry* 11: 528–31.
10. Gibson EM, Geraghty AC, Monje M (2018): Bad wrap: Myelin and myelin plasticity in health and disease. *Developmental Neurobiology* 78: 123–135.
11. Monje M (2018): Myelin Plasticity and Nervous System Function. *Annual Review of Neuroscience* 41: 61–76.
12. Xin W, Chan JR (2020): Myelin plasticity: sculpting circuits in learning and memory. *Nat Rev Neurosci* 21: 682–694.
13. Edgar N, Sibille E (2012): A putative functional role for oligodendrocytes in mood regulation. *Translational Psychiatry* 2: e109-9.
14. Gibson EM, Purger D, Mount CW, Goldstein AK, Lin GL, Wood LS, *et al.* (2014): Neuronal activity promotes oligodendrogenesis and adaptive myelination in the mammalian brain. *Science (New York, NY)* 344: 1252304.
15. Barres BA, Raff MC (1993): Proliferation of oligodendrocyte precursor cells depends on electrical activity in axons. *Nature* 361: 258–260.

16. Marinelli C, Bertalot T, Zusso M, Skaper SD, Giusti P (2016): Systematic Review of Pharmacological Properties of the Oligodendrocyte Lineage. *Front Cell Neurosci* 10. https://doi.org/10.3389/fncel.2016.00027
17. Mitew S, Gobius I, Fenlon LR, McDougall SJ, Hawkes D, Xing YL, *et al.* (2018): Pharmacogenetic stimulation of neuronal activity increases myelination in an axon-specific manner. *Nature Communications* 9: 1–16.
18. Lundgaard I, Luzhynskaya A, Stockley JH, Wang Z, Evans KA, Swire M, *et al.* (2013): Neuregulin and BDNF Induce a Switch to NMDA Receptor-Dependent Myelination by Oligodendrocytes ((B. A. Barres, editor)). *PLoS Biology* 11: e1001743.
19. Long KLP, Breton JM, Barraza MK, Perloff OS, Kaufer D (2021): Hormonal Regulation of Oligodendrogenesis I: Effects Across the Lifespan [no. 2]. *Biomolecules* 11: 283.
20. Steadman PE, Xia F, Ahmed M, Mocle AJ, Penning ARA, Geraghty AC, *et al.* (2020): Disruption of Oligodendrogenesis Impairs Memory Consolidation in Adult Mice. *Neuron* 105: 150-164.e6.
21. McKenzie IA, Ohayon D, Li H, De Faria JP, Emery B, Tohyama K, Richardson WD (2014): Motor skill learning requires active central myelination. *Science* 346: 318–322.
22. Vielkind U, Walencewicz A, Levine JM, Bohn MC (1990): Type II glucocorticoid receptors are expressed in oligodendrocytes and astrocytes. *Journal of Neuroscience Research* 27: 360–373.
23. Matsusue Y, Horii-Hayashi N, Kirita T, Nishi M (2014): Distribution of Corticosteroid Receptors in Mature Oligodendrocytes and Oligodendrocyte Progenitors of the Adult Mouse Brain. *Journal of Histochemistry & Cytochemistry* 62: 211–226.
24. Makinodan M, Rosen KM, Ito S, Corfas G (2012): A critical period for social experience-dependent oligodendrocyte maturation and myelination. *Science (New York, NY)* 337: 1357–60.
25. Liu J, Dietz K, DeLoyht JM, Pedre X, Kelkar D, Kaur J, *et al.* (2012): Impaired adult myelination in the prefrontal cortex of socially isolated mice. *Nature Neuroscience* 15: 1621–1623.
26. Pan S, Mayoral SR, Choi HS, Chan JR, Kheirbek MA (2020): Preservation of a remote fear memory requires new myelin formation [no. 4]. *Nat Neurosci* 23: 487–499.
27. Liu J, Dupree JL, Gacias M, Frawley R, Sikder T, Naik P, Casaccia P (2016): Clemastine Enhances Myelination in the Prefrontal Cortex and Rescues Behavioral Changes in Socially Isolated Mice. *Journal of Neuroscience* 36: 957–962.
28. Breton JM, Barraza M, Hu KY, Frias SJ, Long KLP, Kaufer D (2020): Juvenile exposure to acute traumatic stress leads to long-lasting alterations in grey matter myelination in adult female but not male rats. *bioRxiv* 2020.12.14.422686.

29. Liu J, Dietz K, Hodes GE, Russo SJ, Casaccia P (2018): Widespread transcriptional alternations in oligodendrocytes in the adult mouse brain following chronic stress. *Developmental Neurobiology* 78: 152–162.

30. Bonnefil V, Dietz K, Amatruda M, Wentling M, Aubry AV, Dupree JL, *et al.* (2019): Region-specific myelin differences define behavioral consequences of chronic social defeat stress in mice ((C. Dulac, K.-A. Nave, & M. Schmidt, editors)). *eLife* 8: e40855.

31. Lehmann ML, Weigel TK, Elkahloun AG, Herkenham M (2017): Chronic social defeat reduces myelination in the mouse medial prefrontal cortex. *Scientific Reports* 7: 46548.

32. Ono M, Kikusui T, Sasaki N, Ichikawa M, Mori Y, Murakami-Murofushi K (2008): Early weaning induces anxiety and precocious myelination in the anterior part of the basolateral amygdala of male Balb/c mice. *Neuroscience* 156: 1103–1110.

33. Chetty S, Friedman AR, Taravosh-Lahn K, Kirby ED, Mirescu C, Guo F, *et al.* (2014): Stress and glucocorticoids promote oligodendrogenesis in the adult hippocampus. *Molecular Psychiatry* 19: 1275–1283.

34. Birey F, Kloc M, Chavali M, Hussein I, Wilson M, Christoffel DJ, *et al.* (2015): Genetic and Stress-Induced Loss of NG2 Glia Triggers Emergence of Depressive-like Behaviors through Reduced Secretion of FGF2. *Neuron* 88: 941–956.

35. Sokolov BP (2007): Oligodendroglial abnormalities in schizophrenia, mood disorders and substance abuse. Comorbidity, shared traits, or molecular phenocopies? *The International Journal of Neuropsychopharmacology* 10: 547.

36. Nave K-A, Ehrenreich H (2014): Myelination and Oligodendrocyte Functions in Psychiatric Diseases. *JAMA Psychiatry* 71: 582.

37. Falkai P, Steiner J, Malchow B, Shariati J, Knaus A, Bernstein H-G, *et al.* (2016): Oligodendrocyte and Interneuron Density in Hippocampal Subfields in Schizophrenia and Association of Oligodendrocyte Number with Cognitive Deficits. *Frontiers in Cellular Neuroscience* 10: 1–13.

38. Ma N, Li L, Shu N, Liu J, Gong G, He Z, *et al.* (2007): White Matter Abnormalities in First-Episode, Treatment-Naive Young Adults With Major Depressive Disorder. *American Journal of Psychiatry* 164: 823–826.

39. Hanson JL, Adluru N, Chung MK, Alexander AL, Davidson RJ, Pollak SD (2013): Early neglect is associated with alterations in white matter integrity and cognitive functioning. *Child development* 84: 1566–78.

40. Peirce TR, Bray NJ, Williams NM, Norton N, Moskvina V, Preece A, *et al.* (2006): Convergent Evidence for 2′,3′-Cyclic Nucleotide 3′-Phosphodiesterase as a Possible Susceptibility Gene for Schizophrenia. *Archives of General Psychiatry* 63: 18.

41. Taylor WD, Steffens DC, MacFall JR, McQuoid DR, Payne ME, Provenzale JM, Krishnan KRR (2003): White Matter Hyperintensity Progression and Late-Life Depression Outcomes. *Archives of General Psychiatry* 60: 1090.

42. Bae JN, MacFall JR, Krishnan KRR, Payne ME, Steffens DC, Taylor WD (2006): Dorsolateral Prefrontal Cortex and Anterior Cingulate Cortex White Matter Alterations in Late-Life Depression. *Biological Psychiatry* 60: 1356–1363.

43. Nagy C, Maitra M, Tanti A, Suderman M, Théroux J-F, Davoli MA, *et al.* (2020): Single-nucleus transcriptomics of the prefrontal cortex in major depressive disorder implicates oligodendrocyte precursor cells and excitatory neurons. *Nature Neuroscience* 1–11.

44. Hamidi M, Drevets WC, Price JL (2004): Glial reduction in amygdala in major depressive disorder is due to oligodendrocytes. *Biological Psychiatry* 55: 563–569.

45. Sibille E, Wang Y, Joeyen-Waldorf J, Gaiteri C, Surget A, Oh S, *et al.* (2009): A Molecular Signature of Depression in the Amygdala. *AJP* 166: 1011–1024.

46. Zuo N, Fang J, Lv X, Zhou Y, Hong Y, Li T, *et al.* (2012): White Matter Abnormalities in Major Depression: A Tract-Based Spatial Statistics and Rumination Study ((C. Soriano-Mas, editor)). *PLoS ONE* 7: e37561.

47. Chao LL, Tosun D, Woodward SH, Kaufer D, Neylan TC (2015): Preliminary Evidence of Increased Hippocampal Myelin Content in Veterans with Posttraumatic Stress Disorder. *Frontiers in Behavioral Neuroscience* 9: 1–8.

48. Cohen H, Zohar J (2004): An animal model of posttraumatic stress disorder: the use of cut-off behavioral criteria. *Ann N Y Acad Sci* 1032: 167–178.

49. Schindelin J, Arganda-Carreras I, Frise E, Kaynig V, Longair M, Pietzsch T, *et al.* (2012): *Fiji: An Open-Source Platform for Biological-Image Analysis*. https://doi.org/10.1038/nmeth.2019

50. Fischl B (2012): FreeSurfer. *Neuroimage* 62: 774–781.

51. Zoladz PR, Diamond DM (2016): Predator-based psychosocial stress animal model of PTSD: Preclinical assessment of traumatic stress at cognitive, hormonal, pharmacological, cardiovascular and epigenetic levels of analysis. *Experimental Neurology* 284: 211–219.

52. Morrow BA, Redmond AJ, Roth RH, Elsworth JD (2000): The predator odor, TMT, displays a unique, stress-like pattern of dopaminergic and endocrinological activation in the rat. *Brain Res* 864: 146–151.

53. Muroy SE, Long KLP, Kaufer D, Kirby ED (2016): Moderate Stress-Induced Social Bonding and Oxytocin Signaling are Disrupted by Predator Odor in Male Rats. *Neuropsychopharmacology* 41: 2160–2170.

54. COHEN H, ZOHAR J (2004): An Animal Model of Posttraumatic Stress Disorder: The Use of Cut-Off Behavioral Criteria. *Annals of the New York Academy of Sciences* 1032: 167–178.

55. Cohen H, Kozlovsky N, Alona C, Matar MA, Joseph Z (2012): Animal model for PTSD: From clinical concept to translational research. *Neuropharmacology* 62: 715–724.

56. Sturman O, Germain P-L, Bohacek J (2018): Exploratory rearing: a context- and stress-sensitive behavior recorded in the open-field test. *Stress* 21: 443–452.

57. Smolinsky AN, Bergner CL, LaPorte JL, Kalueff AV (2009): Analysis of Grooming Behavior and Its Utility in Studying Animal Stress, Anxiety, and Depression. In: Gould TD, editor. *Mood and Anxiety Related Phenotypes in Mice: Characterization Using Behavioral Tests*. Totowa, NJ: Humana Press, pp 21–36.

58. Cohen H, Zohar J, Matar MA, Zeev K, Loewenthal U, Richter-Levin G (2004): Setting Apart the Affected: The Use of Behavioral Criteria in Animal Models of Post Traumatic Stress Disorder. *Neuropsychopharmacology* 29: 1962–1970.

59. Scher CD, McCreary DR, Asmundson GJG, Resick PA (2008): The structure of post-traumatic stress disorder symptoms in three female trauma samples: A comparison of interview and self-report measures. *J Anxiety Disord* 22: 1137–1145.

60. Cerniauskas I, Winterer J, Jong JW de, Lukacsovich D, Yang H, Khan F, *et al.* (2019): Chronic Stress Induces Activity, Synaptic, and Transcriptional Remodeling of the Lateral Habenula Associated with Deficits in Motivated Behaviors. *Neuron* 104: 899-915.e8.

61. Cohen H, Matar MA, Zohar J (2011): The "Cut-Off Behavioral Criteria" Method: Modeling Clinical Diagnostic Criteria in Animal Studies of PTSD. In: Gould TD, editor. *Mood and Anxiety Related Phenotypes in Mice: Characterization Using Behavioral Tests, Volume II*. Totowa, NJ: Humana Press, pp 185–208.

62. Cohen S, Matar MA, Vainer E, Zohar J, Kaplan Z, Cohen H (2020): Significance of the orexinergic system in modulating stress-related responses in an animal model of post-traumatic stress disorder. *Transl Psychiatry* 10. https://doi.org/10.1038/s41398-020-0698-9

63. Jovanovic T, Ressler KJ (2010): How the Neurocircuitry and Genetics of Fear Inhibition May Inform Our Understanding of PTSD. *AJP* 167: 648–662.

64. Jovanovic T, Kazama A, Bachevalier J, Davis M (2012): Impaired safety signal learning may be a biomarker of PTSD. *Neuropharmacology* 62: 695–704.

65. King DW, Leskin GA, King LA, Weathers FW (1998): Confirmatory factor analysis of the clinician-administered PTSD Scale: Evidence for the dimensionality of posttraumatic stress disorder. *Psychological Assessment* 10: 90–96.

66. Yehuda R (2002): Post-Traumatic Stress Disorder. *New England Journal of Medicine* 346: 108–114.

67. Horovitz O, Tsoory MM, Yovell Y, G Richter-Levin (2014): A rat model of pre-puberty {(Juvenile)} stress-induced predisposition to stress-related disorders: Sex similarities and sex differences in effects and symptoms. *World J Biol Psychiatry* 15: 36–48.

68. Tsoory M, Richter-Levin G (2006): Learning under stress in the adult rat is differentially affected by "juvenile" or "adolescent" stress. *International Journal of Neuropsychopharmacology* 9: 713–728.

69. Cohen H, Matar MA, Buskila D, Kaplan Z, Zohar J (2008): Early post-stressor intervention with high-dose corticosterone attenuates posttraumatic stress response in an animal model of posttraumatic stress disorder. *Biol Psychiatry* 64: 708–717.

70. Kim GS, Uddin M (2020): Sex-specific and shared expression profiles of vulnerability and resilience to trauma in brain and blood. *Biology of Sex Differences* 11: 13.

71. Kheirbek MA, Drew LJ, Burghardt NS, Costantini DO, Tannenholz L, Ahmari SE, *et al.* (2013): Differential Control of Learning and Anxiety along the Dorsoventral Axis of the Dentate Gyrus. *Neuron* 77: 955–968.

72. McNaughton N, Gray JA (2000): Anxiolytic action on the behavioural inhibition system implies multiple types of arousal contribute to anxiety. *Journal of Affective Disorders* 61: 161–176.

73. Tempesta D, Mazza M, Iaria G, De Gennaro L, Ferrara M (2012): A specific deficit in spatial memory acquisition in post-traumatic stress disorder and the role of sleep in its consolidation. *Hippocampus* 22: 1154–1163.

74. Maren S, Phan KL, Liberzon I (2013): The contextual brain: implications for fear conditioning, extinction and psychopathology. *Nature reviews Neuroscience* 14: 417–28.

75. Sims KS, Williams RS (1990): The human amygdaloid complex: A cytologic and histochemical atlas using Nissl, myelin, acetylcholinesterase and nicotinamide adenine dinucleotide phosphate diaphorase staining. *Neuroscience* 36: 449–472.

76. Zikopoulos B, John YJ, García-Cabezas MÁ, Bunce JG, Barbas H (2016): The intercalated nuclear complex of the primate amygdala. *Neuroscience* 330: 267–290.

77. Amaral DG, Scharfman HE, Lavenex P (2007): The dentate gyrus: fundamental neuroanatomical organization (dentate gyrus for dummies). *Progress in Brain Research*, vol. 163. pp 3–790.

78. Amaral D, Lavenex P (2006): Hippocampal Neuroanatomy ((P. Andersen, R. Morris, D. Amaral, T. Bliss, & J. O'Keefe, editors)). *The Hippocampus Book* 37–114.

79. Ábrahám H, Vincze A, Jewgenow I, Veszprémi B, Kravják A, Gömöri É, Seress L (2010): Myelination in the human hippocampal formation from midgestation to adulthood. *International Journal of Developmental Neuroscience* 28: 401–410.

80. Buzsáki G, Moser EI (2013): Memory, navigation and theta rhythm in the hippocampal-entorhinal system. *Nature Neuroscience* 16: 130–138.

81. Geracioti TD, Baker DG, Ekhator NN, West SA, Hill KK, Bruce AB, *et al.* (2001): CSF Norepinephrine Concentrations in Posttraumatic Stress Disorder. *American Journal of Psychiatry* 158: 1227–1230.

82. Zitnik GA, Curtis AL, Wood SK, Arner J, Valentino RJ (2016): Adolescent Social Stress Produces an Enduring Activation of the Rat Locus Coeruleus and Alters its Coherence with the Prefrontal Cortex. *Neuropsychopharmacology* 41: 1376–1385.

83. Freund TF, Gulyas AI, Acsady L, Gorcs T, Toth K (1990): Serotonergic control of the hippocampus via local inhibitory interneurons. *Proceedings of the National Academy of Sciences* 87: 8501–8505.

84. McKenna JT, Vertes RP (2001): Collateral projections from the median raphe nucleus to the medial septum and hippocampus. *Brain Research Bulletin* 54: 619–630.

85. Dale E, Pehrson AL, Jeyarajah T, Li Y, Leiser SC, Smagin G, *et al.* (2016): Effects of serotonin in the hippocampus: how SSRIs and multimodal antidepressants might regulate pyramidal cell function. *CNS Spectrums* 21: 143–161.

86. Jang M, Gould E, Xu J, Kim EJ, Kim JH (2019): Oligodendrocytes regulate presynaptic properties and neurotransmission through BDNF signaling in the mouse brainstem ((D. E. Bergles, G. L. Westbrook, & L.-Y. Wang, editors)). *eLife* 8: e42156.

87. Yamazaki Y, Hozumi Y, Kaneko K, Sugihara T, Fujii S, Goto K, Kato H (2007): Modulatory effects of oligodendrocytes on the conduction velocity of action potentials along axons in the alveus of the rat hippocampal CA1 region. *Neuron Glia Biology* 3: 325–334.

88. Yamazaki Y, Fujiwara H, Kaneko K, Hozumi Y, Xu M, Ikenaka K, *et al.* (2014): Short- and long-term functional plasticity of white matter induced by oligodendrocyte depolarization in the hippocampus. *Glia* 62: 1299–1312.

89. Fields RD (2008): Oligodendrocytes Changing the Rules: Action Potentials in Glia and Oligodendrocytes Controlling Action Potentials. *The Neuroscientist* 14: 540–543.

90. Fields RD (2015): A new mechanism of nervous system plasticity: activity-dependent myelination [no. 12]. *Nature Reviews Neuroscience* 16: 756–767.

91. Christiansen DM, Berke ET (2020): Gender- and Sex-Based Contributors to Sex Differences in PTSD. *Curr Psychiatry Rep* 22: 19.

92. Tolin DF, Foa EB (2006): Sex differences in trauma and posttraumatic stress disorder: A quantitative review of 25 years of research. *Psychological Bulletin* 132: 959–992.

93. Pooley AE, Benjamin RC, Sreedhar S, Eagle AL, Robison AJ, Mazei-Robison MS, *et al.* (2018): Sex differences in the traumatic stress response: the role of adult gonadal hormones. *Biology of Sex Differences* 9: 32.

94. Goudriaan A, de Leeuw C, Ripke S, Hultman CM, Sklar P, Sullivan PF, *et al.* (2014): Specific Glial Functions Contribute to Schizophrenia Susceptibility. *Schizophr Bull* 40: 925–935.

95. Travers BG, Adluru N, Ennis C, Tromp DPM, Destiche D, Doran S, *et al.* (2012): Diffusion Tensor Imaging in Autism Spectrum Disorder: A Review. *Autism Research* 5: 289–313.

96. Nasrabady SE, Rizvi B, Goldman JE, Brickman AM (2018): White matter changes in Alzheimer's disease: a focus on myelin and oligodendrocytes. *Acta Neuropathol Commun* 6. https://doi.org/10.1186/s40478-018-0515-3

97. Breton J, Long K, Barraza M, Litvin O, Kaufer D (2021): Hormonal Regulation of Oligodendrogenesis II: Implications for Myelin Repair. https://doi.org/10.20944/preprints202101.0282.v1

Figures:

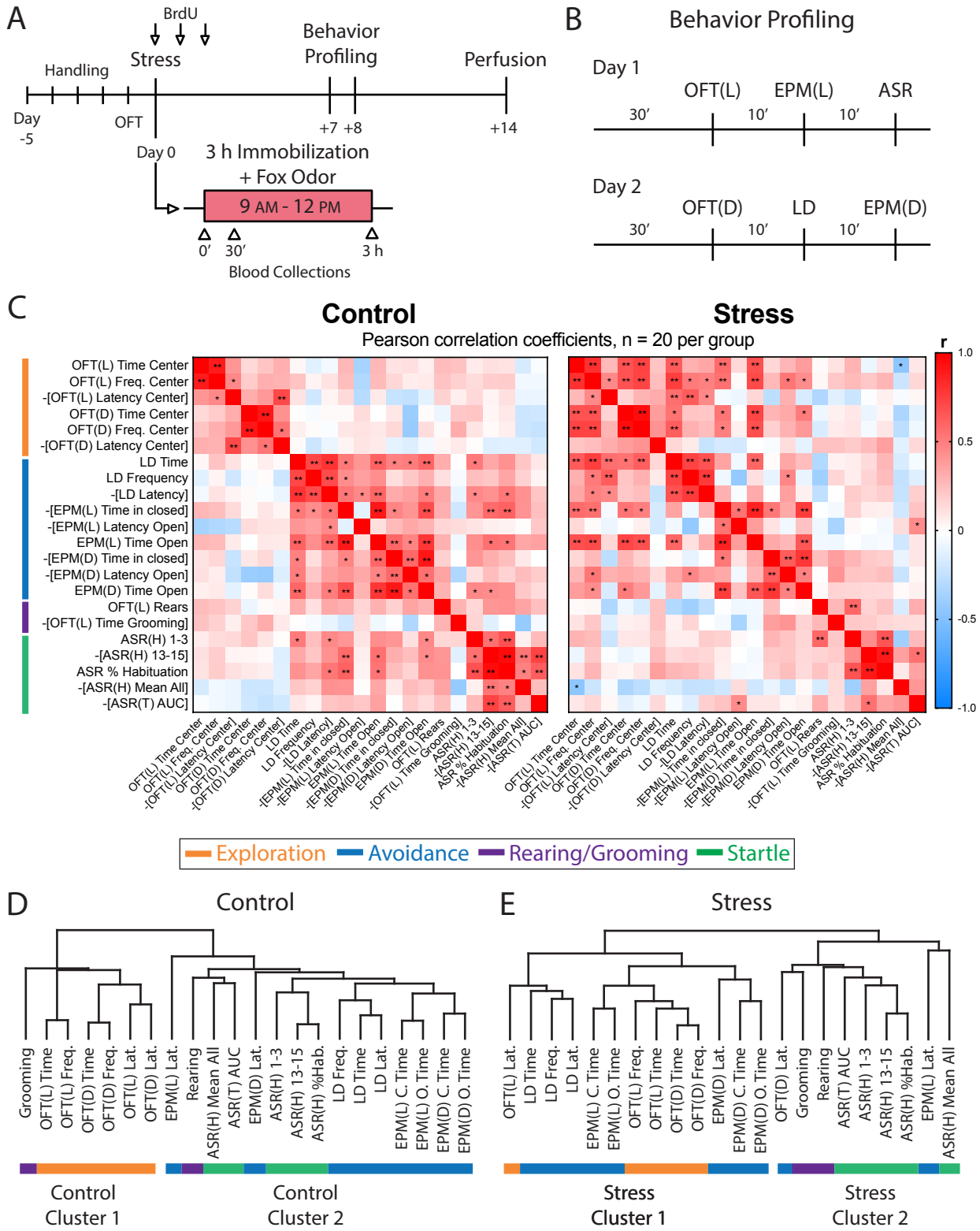

Fig. 1: Acute, severe stress alters individual profiles of exploration, avoidance, and startle behavior

in male rats. (A) Experimental design. BrdU, bromodeoxyuridine. **(B)** Two-day behavior profiling design. OFT(L), open field test under bright light; OFT(D), open field test under dim light; EPM(L), elevated plus maze under bright light; EPM(D), elevated plus maze under dim light; ASR, acoustic startle response; LD, light-dark box. **(C)** Correlation matrices of behavioral measures from control and stress-exposed groups. Pearson r values are represented with red as positive and blue as negative. For ease of interpretation, latency measures, time spent in anxiolytic zones, etc. were negated to maintain a consistent directionality of valence (e.g. –[LD Latency]). **(D-E)** Hierarchical clustering of behavioral measures for control (D) and stress-exposed (E) animals. OFT measures: Time, time in center; Freq., frequency in center; Lat., latency to center. EPM measures: Lat., latency to open arm; C. Time, time in closed arm; O. Time, time in open arm. LD measures: Time, time in open zone; Freq., frequency in open zone; Lat., latency to open zone. ASR(H), ASR habituation phase: Mean All, mean startle to all 15 110 dB stimuli; 1-3, average startle to stimuli 1-3; 13-15, average startle to stimuli 13-15; %Hab., percent habituation. ASR(T) AUC, ASR threshold phase area under the curve. *$p < 0.05$, **$p < 0.01$; n = 20 for all comparisons.

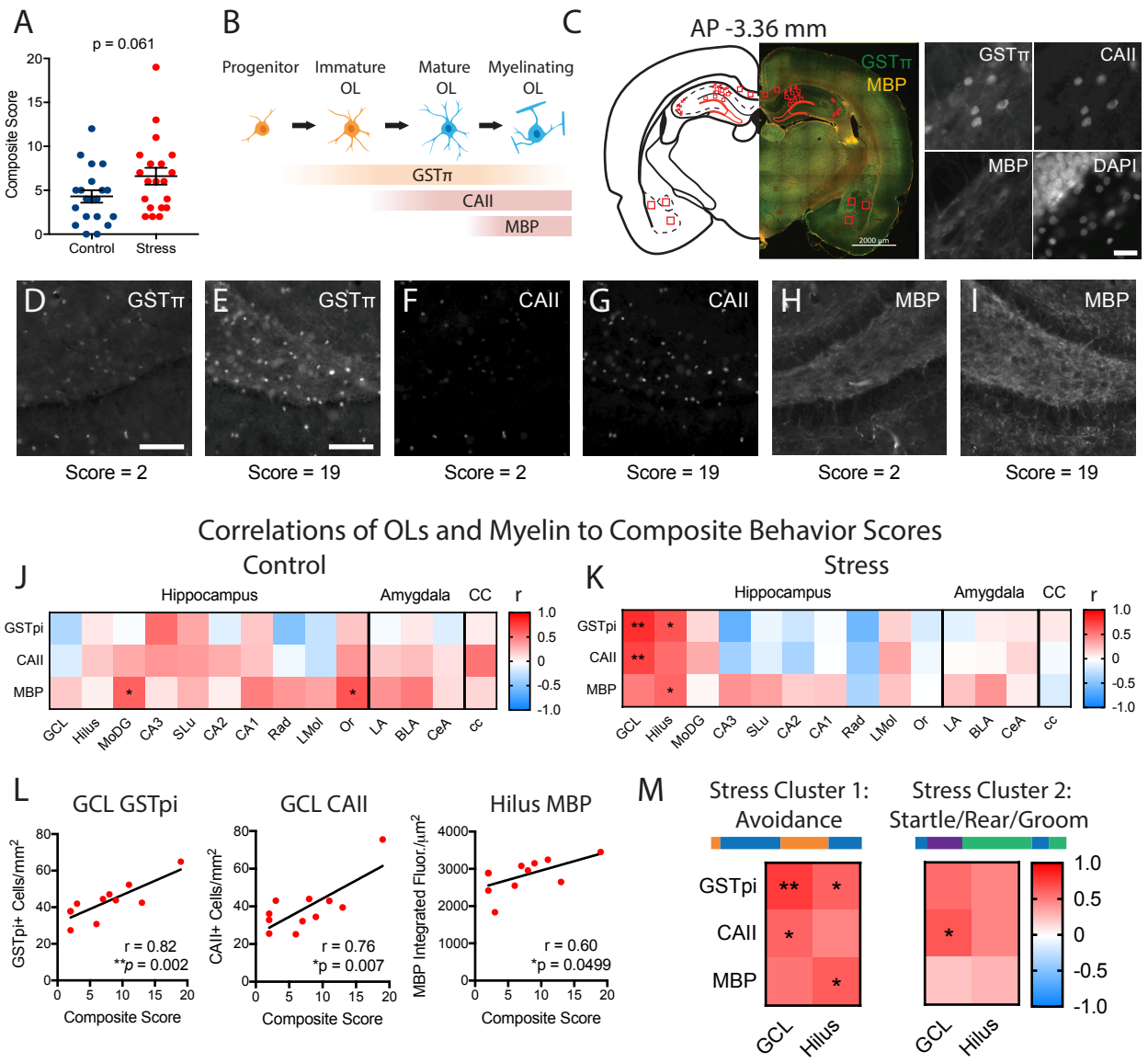

Fig. 2: DG oligodendrocytes and myelin are positively correlated with anxiety-like and avoidance behavior after acute stress. (A) Composite scores of anxiety-like behavior from all tests (mean ± SEM; Control: 4.3 ± 0.7, Stress: 6.6 ± 1.0; two-tailed t test: $t_{2,38} = 1.94$, $p = 0.061$; n = 20 per group). **(B)** Markers for immature and mature oligodendrocytes (OLs) and myelin selected for immunohistochemical analysis: GSTπ, glutathione S-transferase pi; CAII, carbonic anhydrase II; MBP, myelin basic protein; DAPI, 4′,6-diamidino-2-phenylindole. **(C)** Left: Example coronal section with hippocampal, amygdala, and corpus callosum ROIs indicated in red. Right: Representative GSTπ, CAII, and MBP staining. Scale bar = 20 µm. **(D-I)** Representative images of each oligodendrocyte marker from animals with low (composite score = 2) or high (composite score = 19) composite behavior scores. Scale bar = 100 µm. **(J,K)** Correlation matrices of composite behavior scores to oligodendrocyte and myelin measures from a subset of control (J) and

stress-exposed (K) animals spanning composite scores (Pearson correlations: $n_{Control}$ = 11-12, n_{Stress} = 10-11). **(L)** Correlation plots from stress-exposed animals of oligodendrocytes and myelin to composite behavior scores [Pearson correlations of composite scores to GCL GSTπ (r = 0.82, p = 0.002), GCL CAII (r = 0.76, p = 0.007), and hilus MBP (r = 0.60, p = 0.0499), n = 11]. **(M)** Correlation matrices of DG oligodendrocytes and myelin from stress-exposed animals to composite scores derived from hierarchical behavior clustering (Pearson correlations: n = 11). *p < 0.05, **p < 0.01.

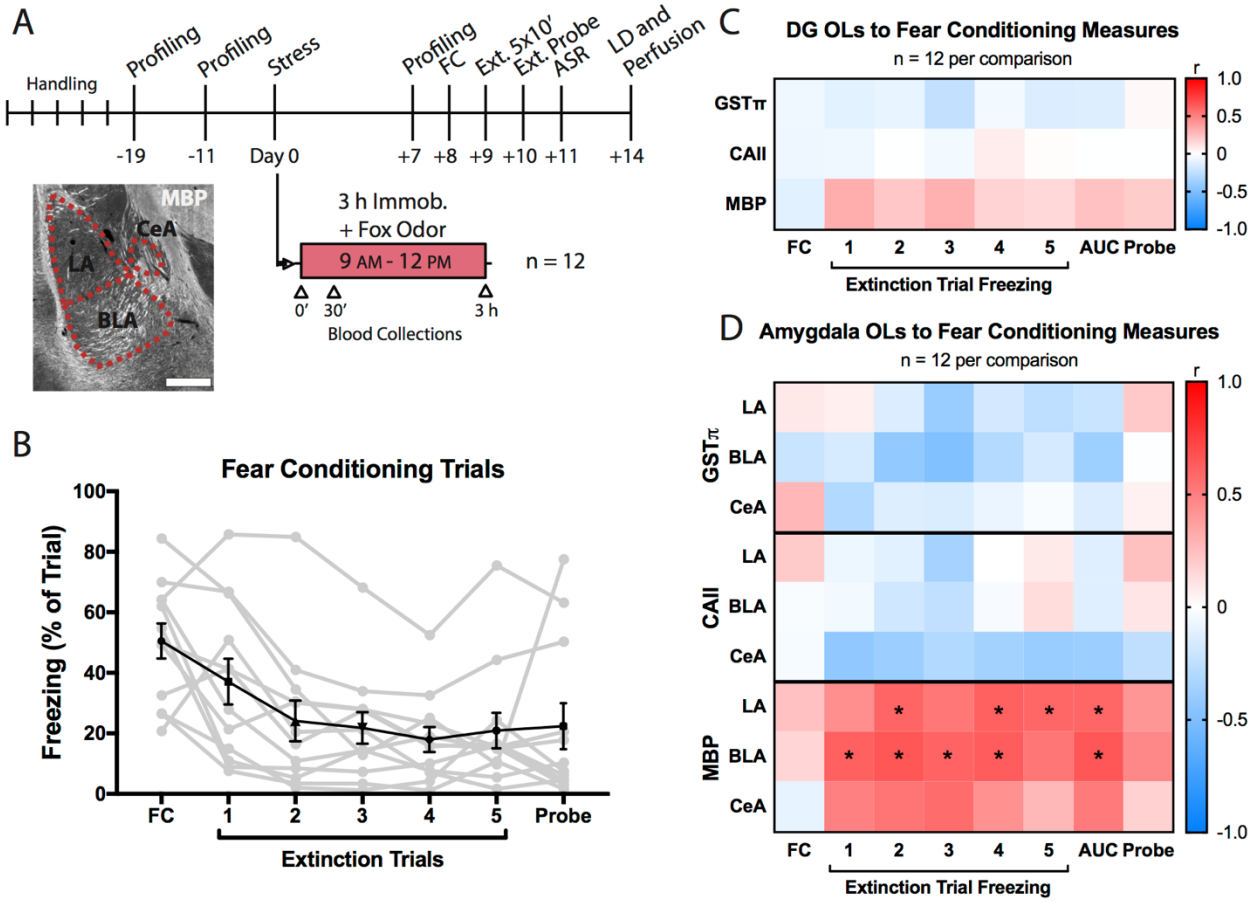

Fig. 3: Amygdala myelin, but not oligodendrocyte content, is positively correlated with fear outcomes after acute stress in male rats. (A) Experimental design. Inset image: Representative MBP staining with amygdala ROIs outlined in red: Lateral amygdala (LA), basolateral amygdala (BLA), central amygdala (CeA). Scale bar = 450 µm. **(B)** Freezing across fear conditioning trials as percent of total trial time. Individual animals are shown in gray with mean ± SEM freezing of all 12 animals shown in black. FC, Fear conditioning. **(C)** Correlation matrix of dentate gyrus (DG) oligodendrocyte markers to freezing behavior from fear conditioning (FC), extinction trials, area under the curve (AUC) of extinction freezing traces, and

the probe trial (Pearson correlations: n = 12). **(D)** Correlation matrix of amygdala oligodendrocyte markers to freezing behavior (Pearson correlations: n = 12, *$p < 0.05$).

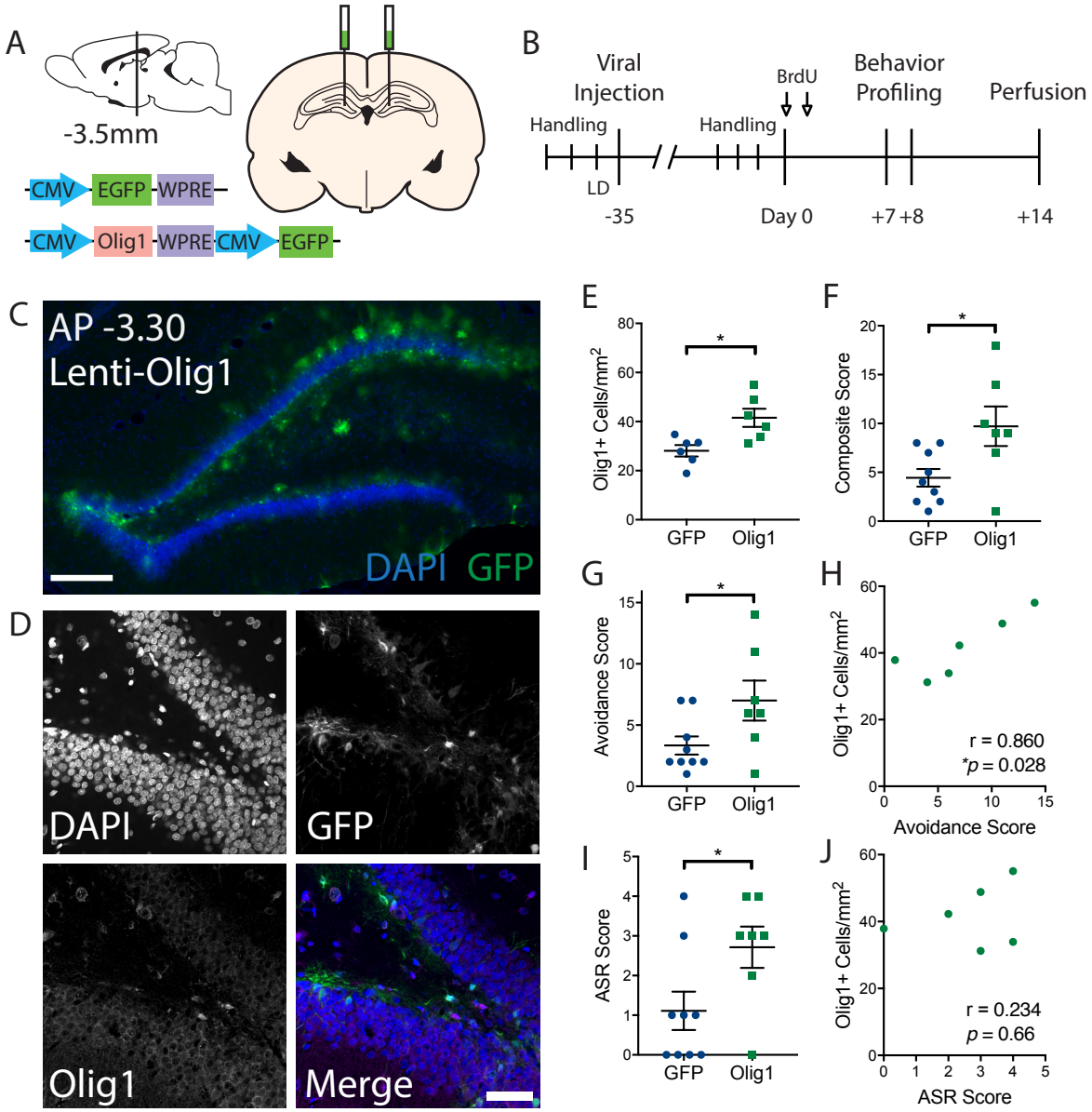

Fig. 4: Viral upregulation of Olig1 in the DG mimics the effects of acute stress. (A) Injection schematic and lentiviral constructs. CMV, human cytomegalovirus promoter; EGFP, enhanced green fluorescent protein; WPRE, Woodchuck hepatitis virus posttranscriptional regulatory element; Olig1, oligodendrocyte transcription factor 1. **(B)** Experimental timeline. BrdU, bromodeoxyuridine; LD, light-dark box. **(C)** Representative image of viral spread through the dorsal DG. Lenti, lentivirus; DAPI, 4′,6-diamidino-2-phenylindole; GFP, green fluorescent protein. Scale bar = 200 µm. **(D)** Representative images of GFP and Olig1 immunohistochemistry 7 weeks post-injection. Scale bar = 50 µm. **(E)** DG Olig1 cell densities (GFP:

28.11 ± 2.33, Olig1: 41.54 ± 3.72; two-tailed t test: $t_{2,10} = 3.06$, $p = 0.012$; n = 6 per group). **(F)** Composite behavior scores (GFP: 4.4 ± 0.9, Olig1: 9.7 ± 2.0; two-tailed t test: $t_{2,14} = 2.58$, $p = 0.022$; $n_{GFP} = 9$, $n_{Olig1} = 7$). **(G)** Composite behavior scores from avoidance tests (GFP: 3.3 ± 0.7, Olig1: 7.0 ± 1.6; two-tailed t test: $t_{2,14} = 2.21$, $p = 0.044$; $n_{GFP} = 9$, $n_{Olig1} = 7$). **(H)** Pearson correlation of Olig1 cell densities to avoidance composite scores from Lenti-Olig1 animals (Pearson correlation: r = 0.86, $p = 0.028$; n = 6). **(I)** Composite behavior scores from the acoustic startle response (ASR) test (GFP: 1.1 ± 0.5, Olig1: 2.7 ± 0.5; two-tailed t test: $t_{2,14} = 2.24$, $p = 0.042$; $n_{GFP} = 9$, $n_{Olig1} = 7$). **(J)** Pearson correlation of Olig1 cell densities to composite startle scores from Lenti-Olig1 animals (Pearson correlation: r = 0.23, $p = 0.66$; n = 6). For all plots, individual data points are shown with mean ± SEM, *$p < 0.05$.

	Hippocampus	**Amygdala**	**Corpus Callosum**
Total CAPS	**0.38***	**0.36***	0.15
Avoidance Sub-score	**0.39***	**0.40***	0.20
Avoidance of thoughts, feelings, conversations	0.27	**0.39***	0.09
Avoidance of activities, places, people	**0.38***	0.30	0.16
Inability to recall aspects of trauma	0.07	0.20	0.04
Diminished interest in activities	**0.33***	**0.35***	0.16
Detachment or estrangement	0.20	0.14	0.09
Restricted affect	**0.39***	0.24	0.25
Sense of foreshortened future	0.26	0.29	0.20
Reexperiencing Sub-score	0.25	0.30	0.11
Intrusive recollection	0.04	0.06	0.09
Distressing dreams	0.26	0.22	0.02
Flashbacks	0.01	0.06	0.15
Psychological distress at exposure to cues	0.29	**0.52****	0.15
Physiological distress at exposure to cues	0.20	**0.38***	0.18
Hyperarousal Sub-score	**0.48****	**0.38***	0.15
Difficulty sleeping	**0.45****	0.31	0.12
Irritability, frequency	**0.56****	0.28	0.06
Difficulty concentrating	**0.35***	0.29	0.05
Hypervigilance	0.15	0.17	0.03
Exaggerated startle response	0.26	**0.33***	0.03

Table 1: Correlations of human regional myelin estimates to sub-components of the Clinician Administered PTSD Scale (CAPS). Myelin estimates were measured via T1/T2-weighted imaging from 38 trauma-exposed male veterans, as described in Chao *et al.*, 2015. 19 trauma-exposed veterans were diagnosed with PTSD, while 19 were PTSD-. All analyses are Spearman's Rank-Order correlations (*$\rho < 0.05$, **$\rho < 0.01$).